Supporting Information

Phosphaguanidinate Yttrium Carbene, Carbyne and Carbide Complexes: Three Distinct C1 Functionalities

Wen Jiang,[a] Lixin Zhang*[a]

[a] Department of Chemistry, Shanghai Key Laboratory of Molecular Catalysis and Innovative Materials, Jiangwan Campus, Fudan University, Shanghai, 200438, China.

Tables of Contents

General. All manipulations were performed with rigorous exclusion of air and water, using Schlenk techniques or an MBRAUN glovebox (Unilab Mbraun; <1 ppm O_2, <1 ppm H_2O). Solvents (toluene, hexane, and THF) were purified using Grubbs-type columns (MBraun SPS-800, solvent purification system), dried over fresh Na chips and stored in glovebox. Bis(2,6-diisopropylphenyl) carbodiimide was obtained from Tokyo Chemical Industry Co., Ltd and used without purification. $CH_3C_6H_4NMe_2$-*o* was purchased from Sigma-Aldrich and used without purification. Ph_2PH and ^nBuLi (2.5 mol L^{-1} in hexane) were purchased from Engery Chemical Co., Ltd and used without purification. The $AlMe_3$ (1 mol L^{-1} in hexane) was purchased from J&K Co., Ltd and used without purification. Benzene-d_6 was obtained from J&K Co., Ltd and dried by using sodium chips. The synthesis of $(Ph_2P)[C(NR)(NHR)]$ (R = 2,6-($^iPr_2$)C_6H_3) refers to reported literature.[1] ^1H, $^{13}C\{^1H\}$, $^{31}P\{^1H\}$, ^{13}C DEPT-135 and ^1H-^{13}C HMQC NMR spectra of complexes were recorded using a JEOL ECA-400 NMR spectrometer (FT, 400 MHz for ^1H; 100 MHz for ^{13}C, 162 MHz for ^{31}P) at room temperature. The combustion method was used for the carbon, hydrogen and nitrogen analyses on an Elementar Vario EL III analyzer at Fudan Univerisity (China).

NMR spectra of all complexes

The solid samples were dissolved in C_6D_6, and then transferred into a J-Young NMR tube in the glove-box. The ^{1}H, $^{13}C\{^{1}H\}$, $^{31}P\{^{1}H\}$, ^{13}C DEPT-135 and ^{1}H-^{13}C HMQC NMR spectra were recorded on a JEOL ECA-400 NMR spectrometer (FT, 400 MHz for ^{1}H; 100 MHz for ^{13}C, 162 MHz for ^{31}P) in C_6D_6 at room temperature.

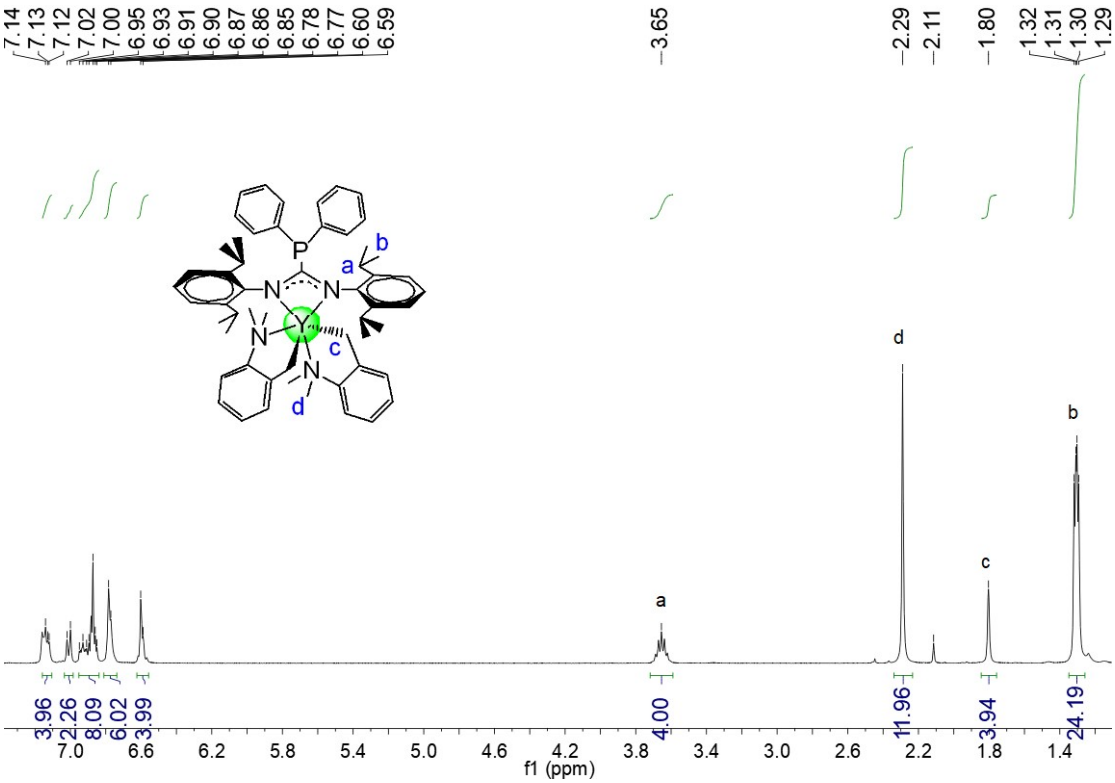

Figure S1. ^{1}H NMR spectrum of **1-Y** obtained in C_6D_6 at room temperature.

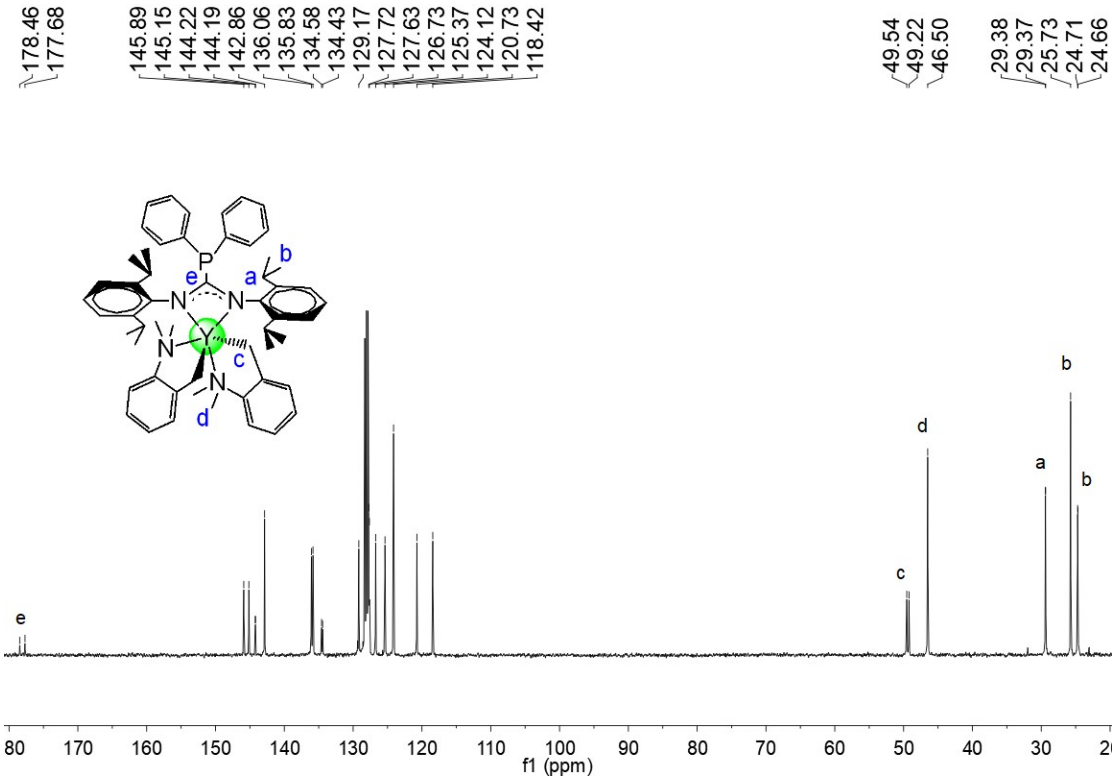

Figure S2. $^{13}C\{^{1}H\}$ NMR spectrum of **1-Y** obtained in C_6D_6 at room temperature.

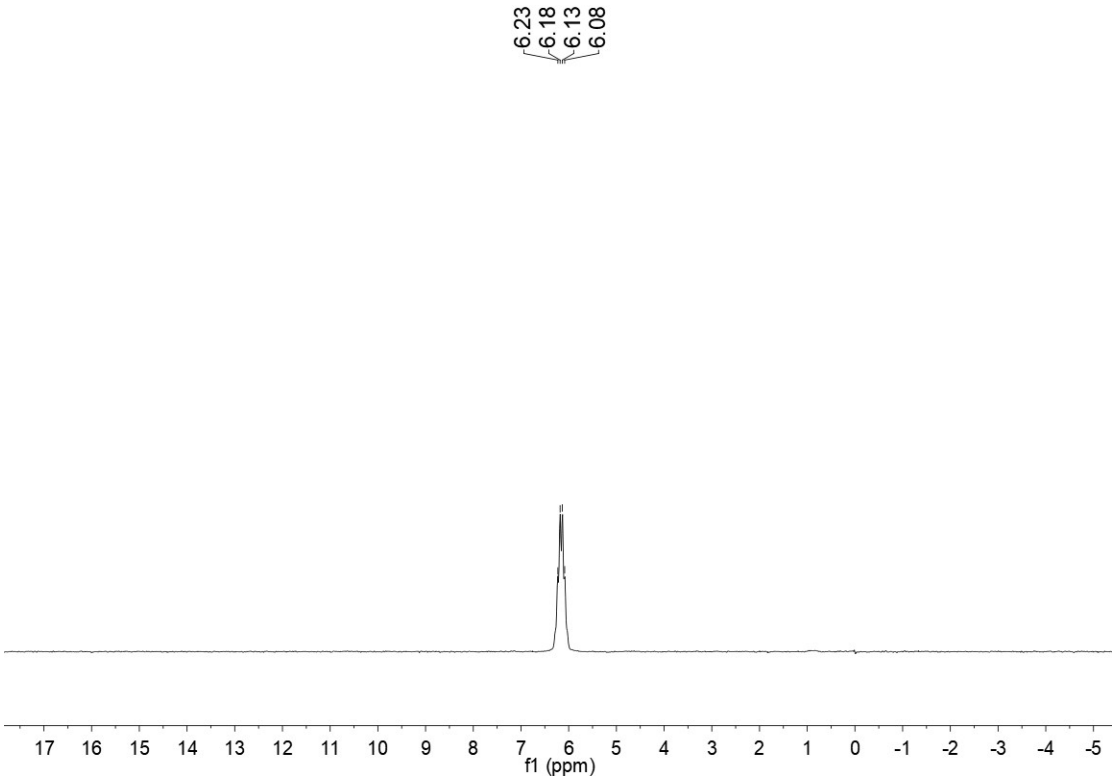

Figure S3. $^{31}P\{^{1}H\}$ NMR spectrum of **1-Y** obtained in C_6D_6 at room temperature.

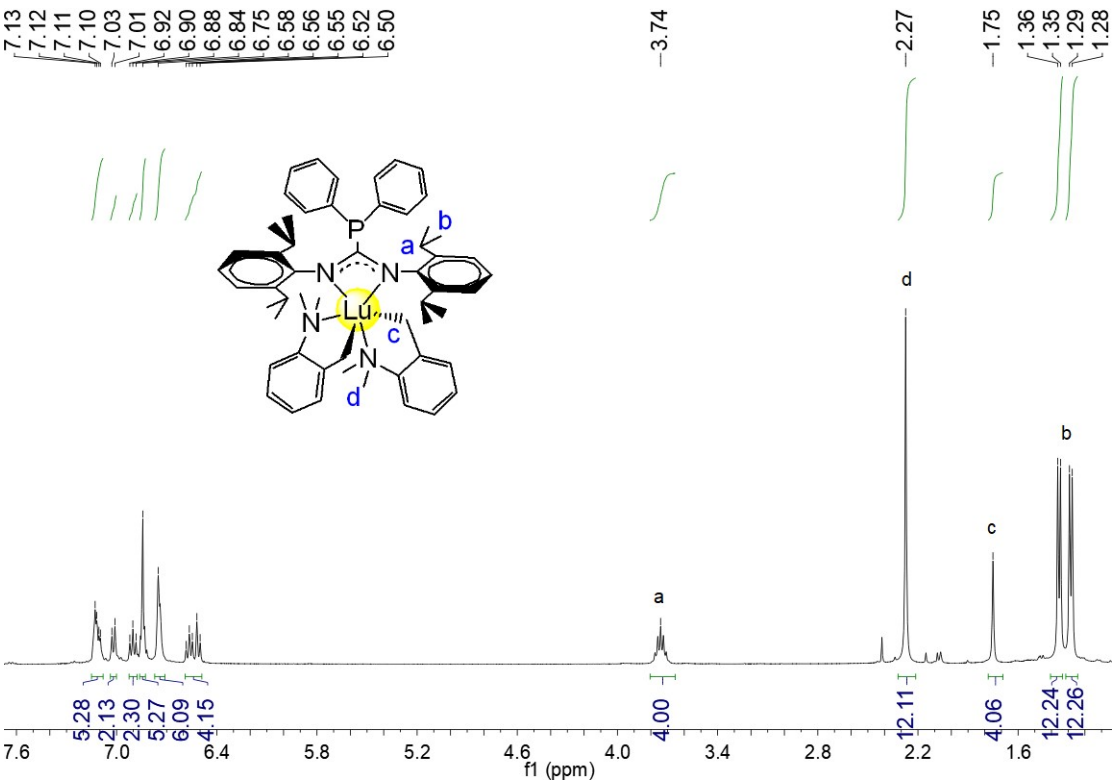

Figure S4. ^{1}H NMR spectrum of **1-Lu** obtained in C_6D_6 at room temperature.

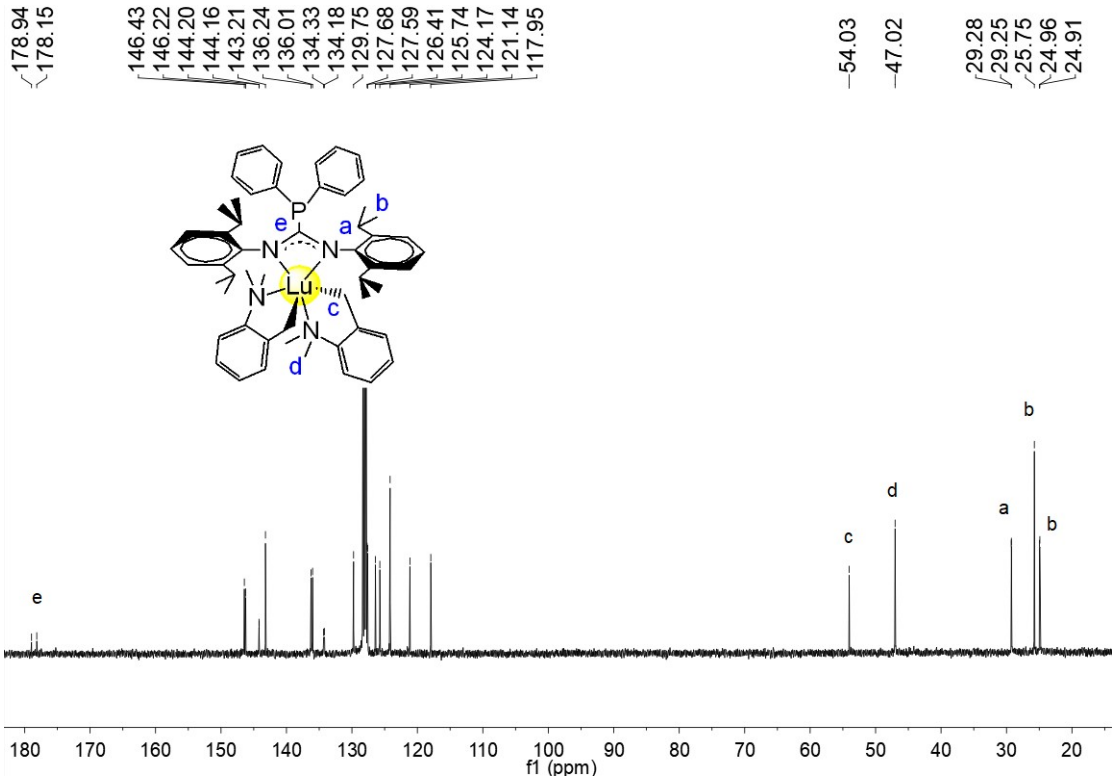

Figure S5. $^{13}C\{^{1}H\}$ NMR spectrum of **1-Lu** obtained in C_6D_6 at room temperature.

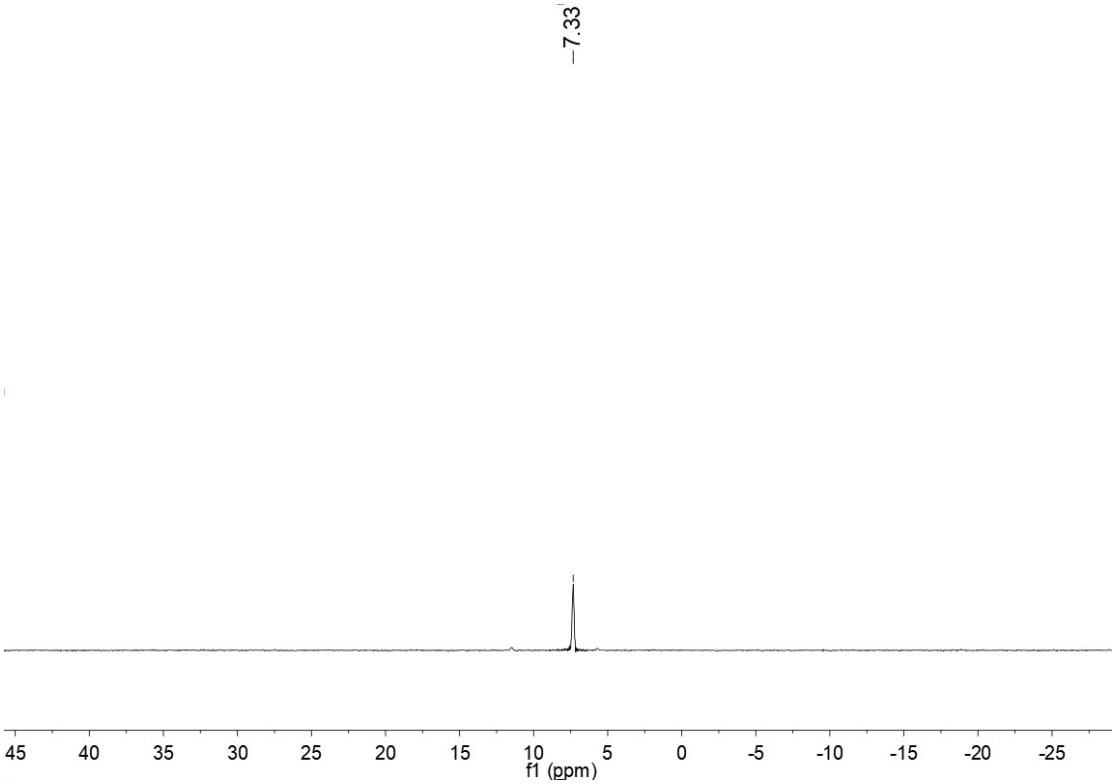

Figure S6. $^{31}P\{^{1}H\}$ NMR spectrum of **1-Lu** obtained in C_6D_6 at room temperature.

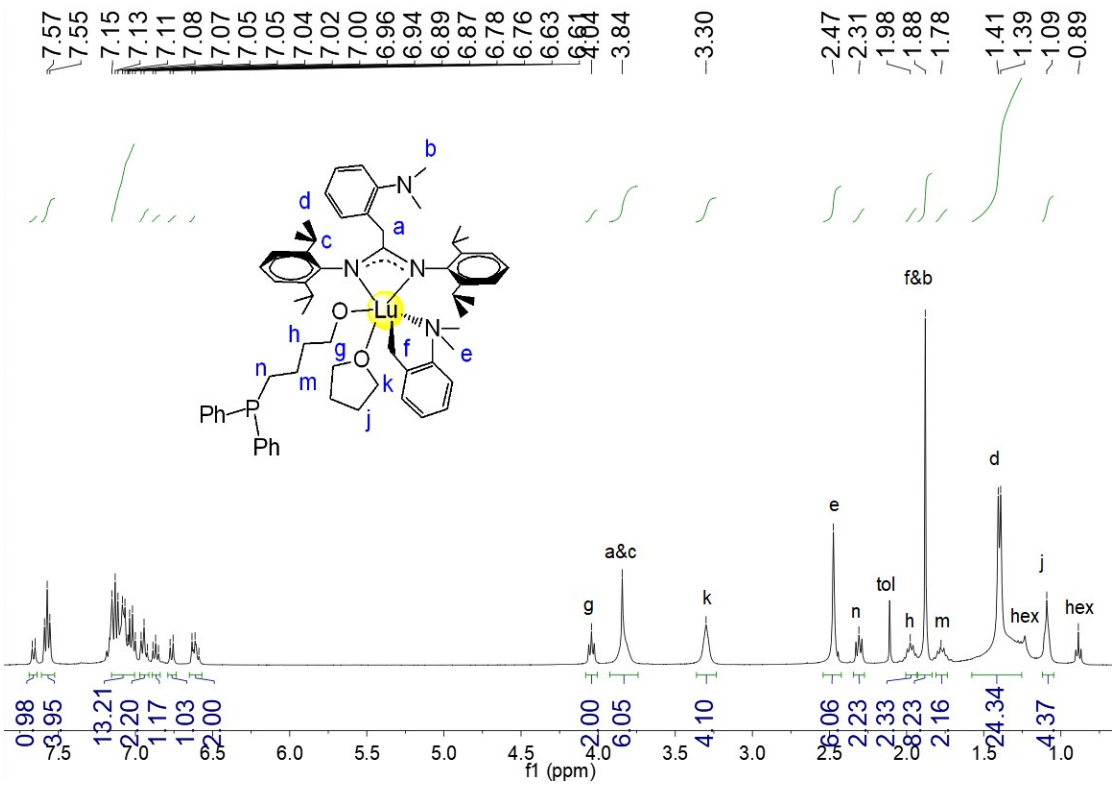

Figure S7. ^{1}H NMR spectrum of **2** obtained in C_6D_6 at room temperature.

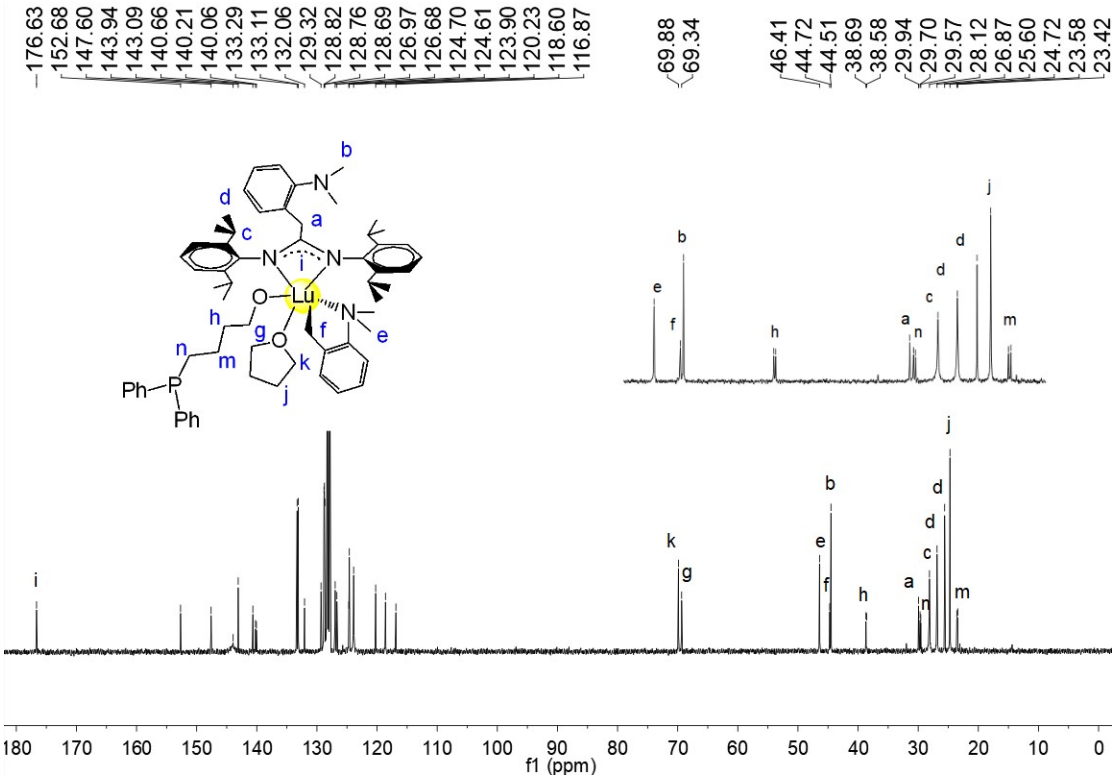

Figure S8. $^{13}C\{^{1}H\}$ NMR spectrum of **2** obtained in C_6D_6 at room temperature.

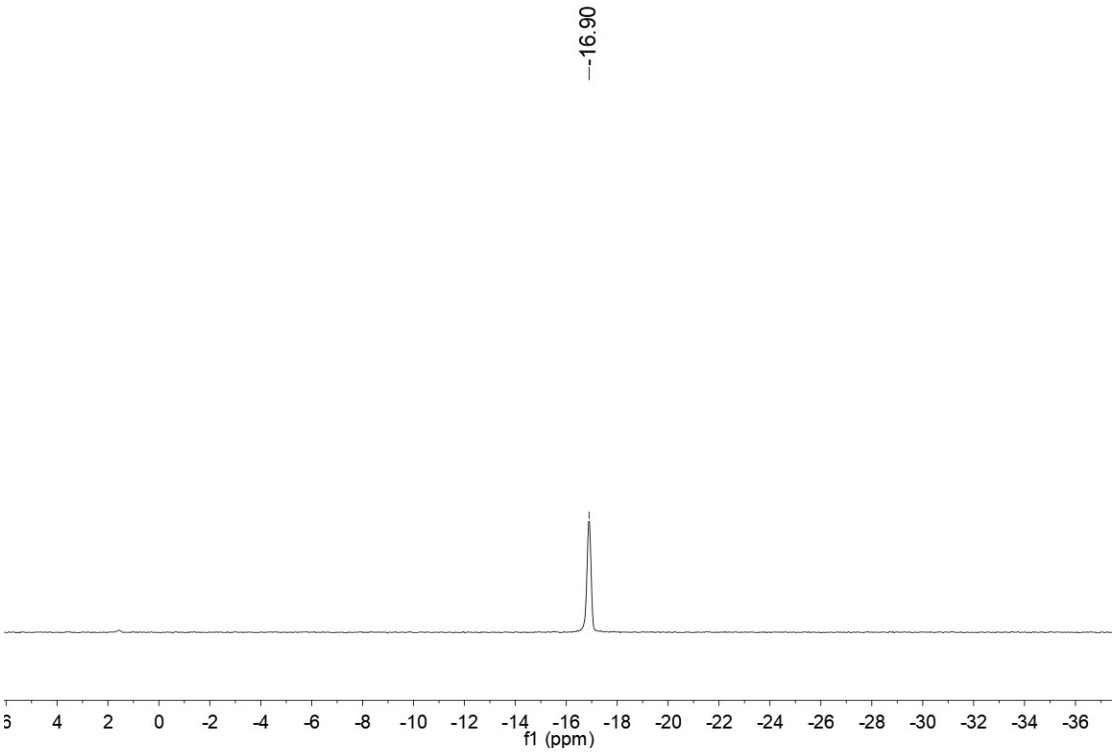

Figure S9. $^{31}P\{^{1}H\}$ NMR spectrum of **2** obtained in C_6D_6 at room temperature.

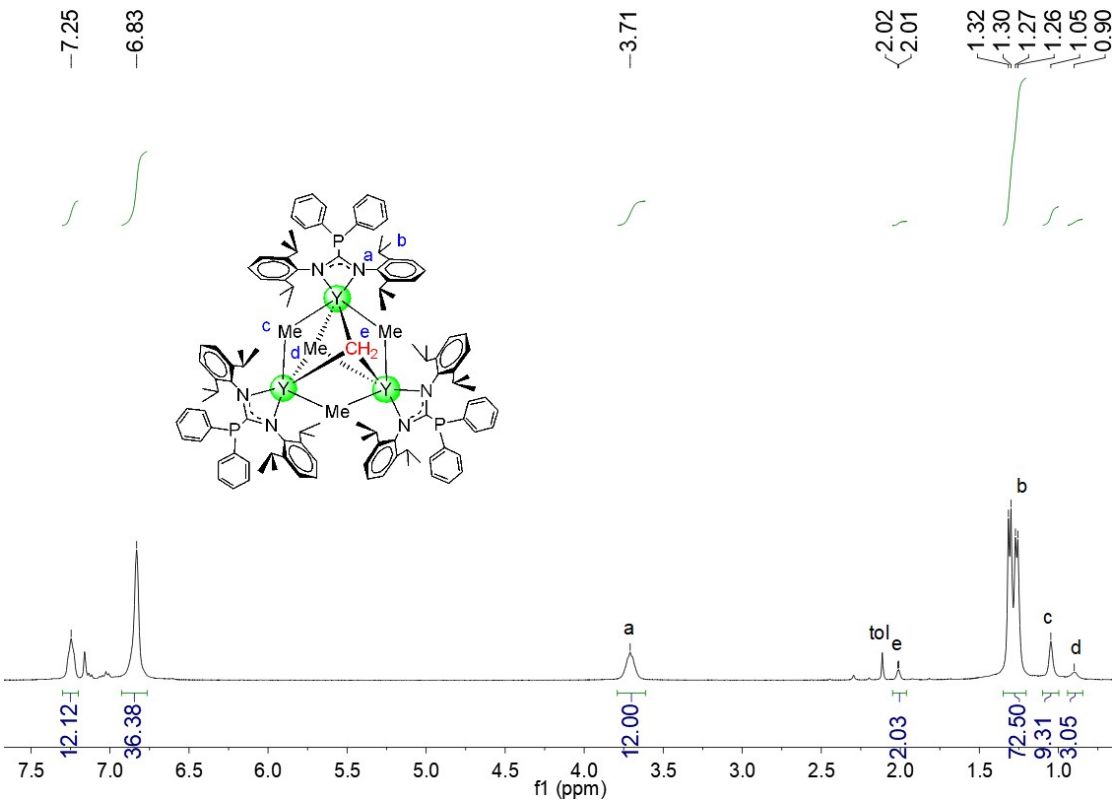

Figure S10. ^{1}H NMR spectrum of **3** obtained in C_6D_6 at room temperature.

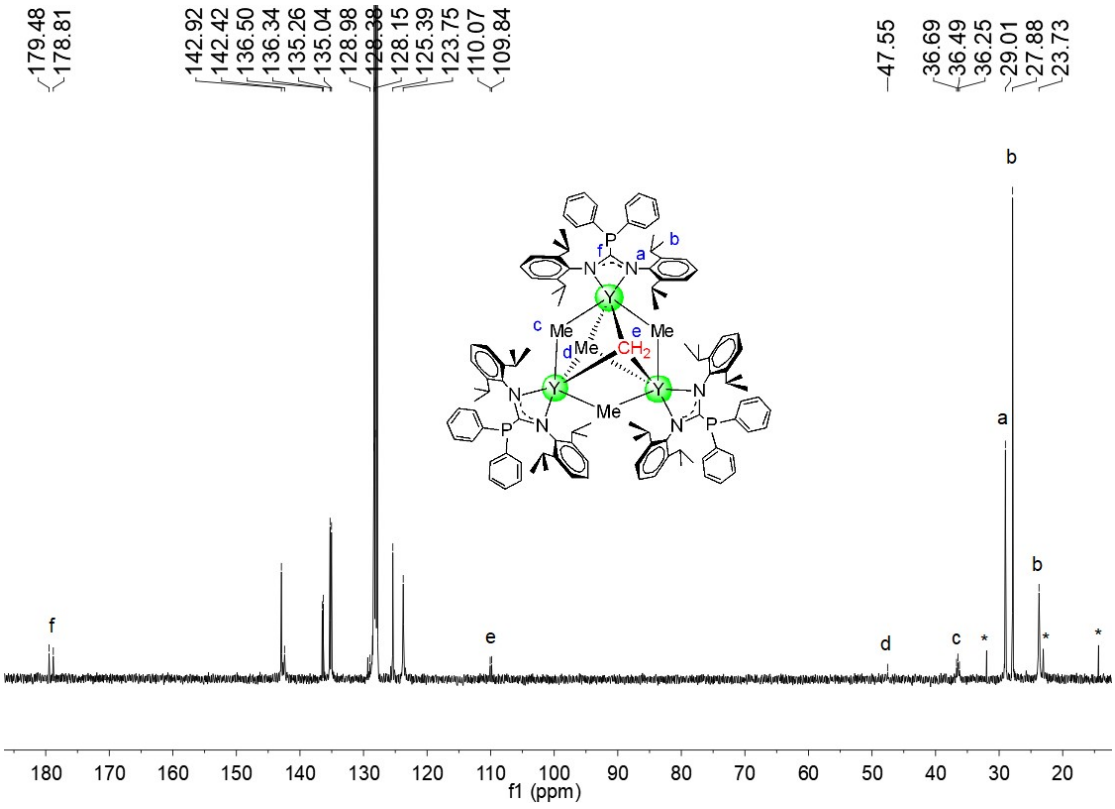

Figure S11. $^{13}C\{^{1}H\}$ NMR spectrum of **3** obtained in C_6D_6 at room temperature.

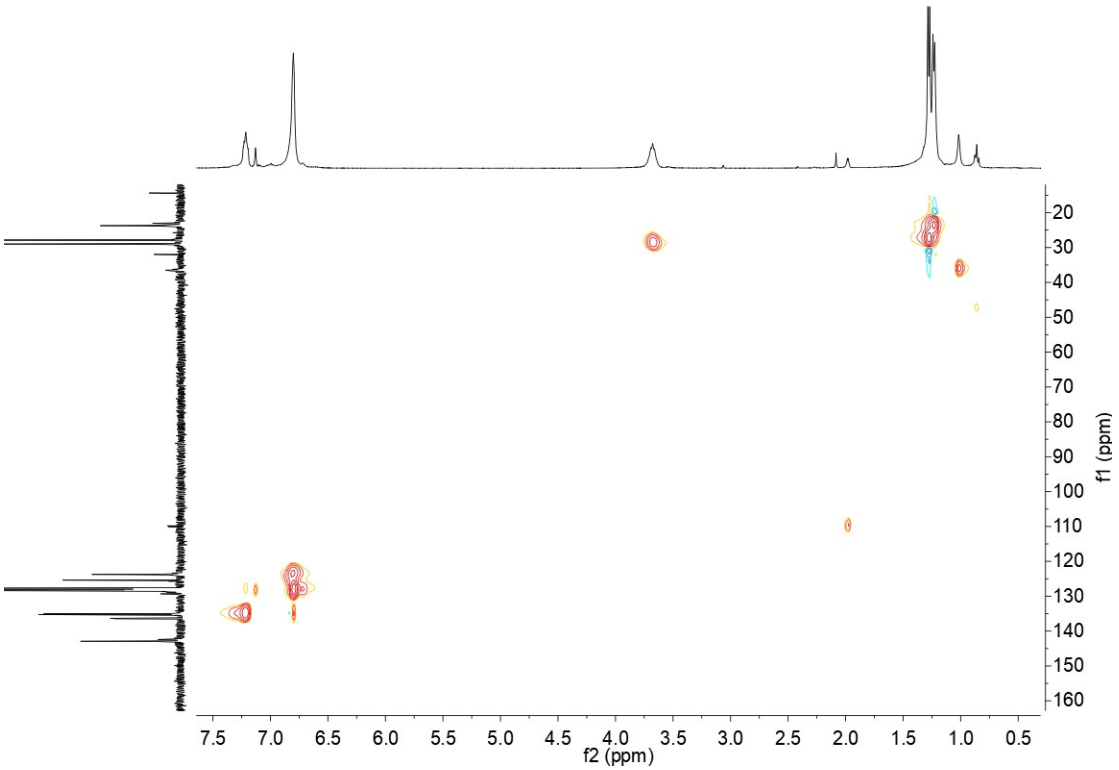

Figure S12. Two-dimensional ^{1}H-^{13}C HMQC NMR spectrum of complex **3** (^{1}H NMR spectrum (400 MHz) on the top, $^{13}C\{^{1}H\}$ NMR spectrum (100 MHz) on the left).

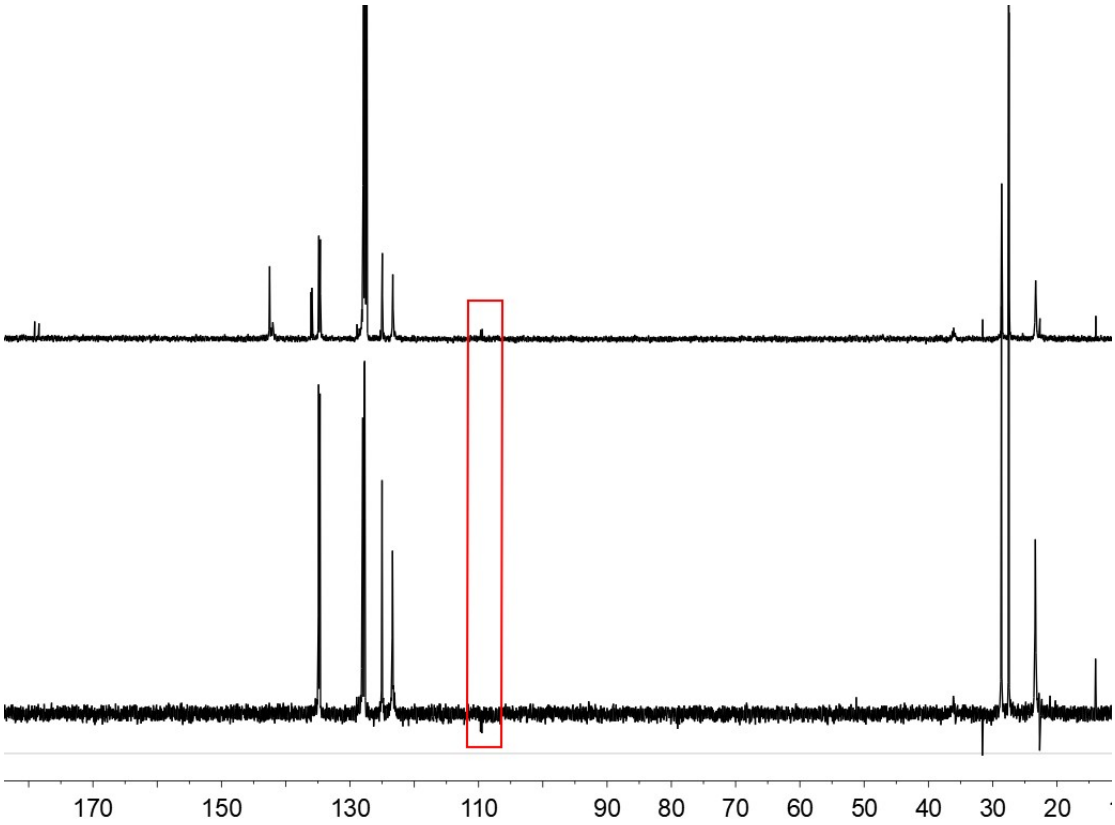

Figure S13. ^{13}C DEPT-135 NMR spectrum of **3** obtained in C_6D_6 at room temperature.

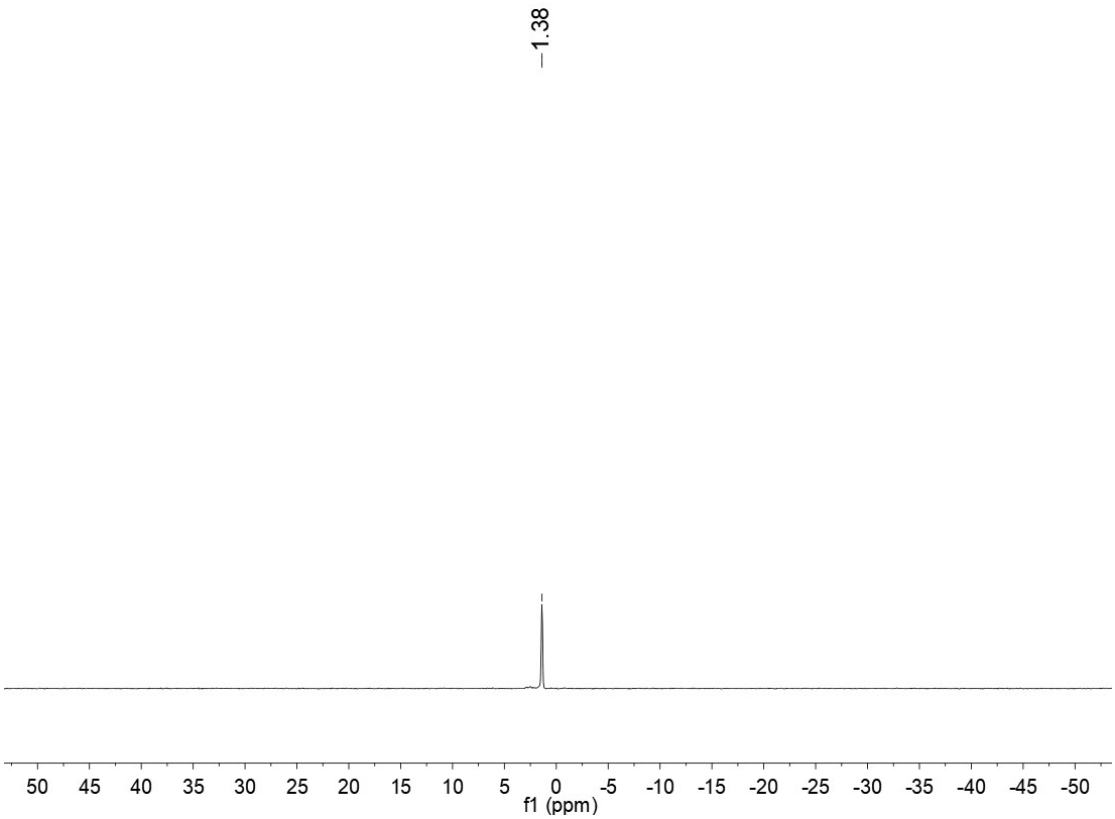

Figure S14. $^{31}P\{^{1}H\}$ NMR spectrum of **3** obtained in C_6D_6 at room temperature.

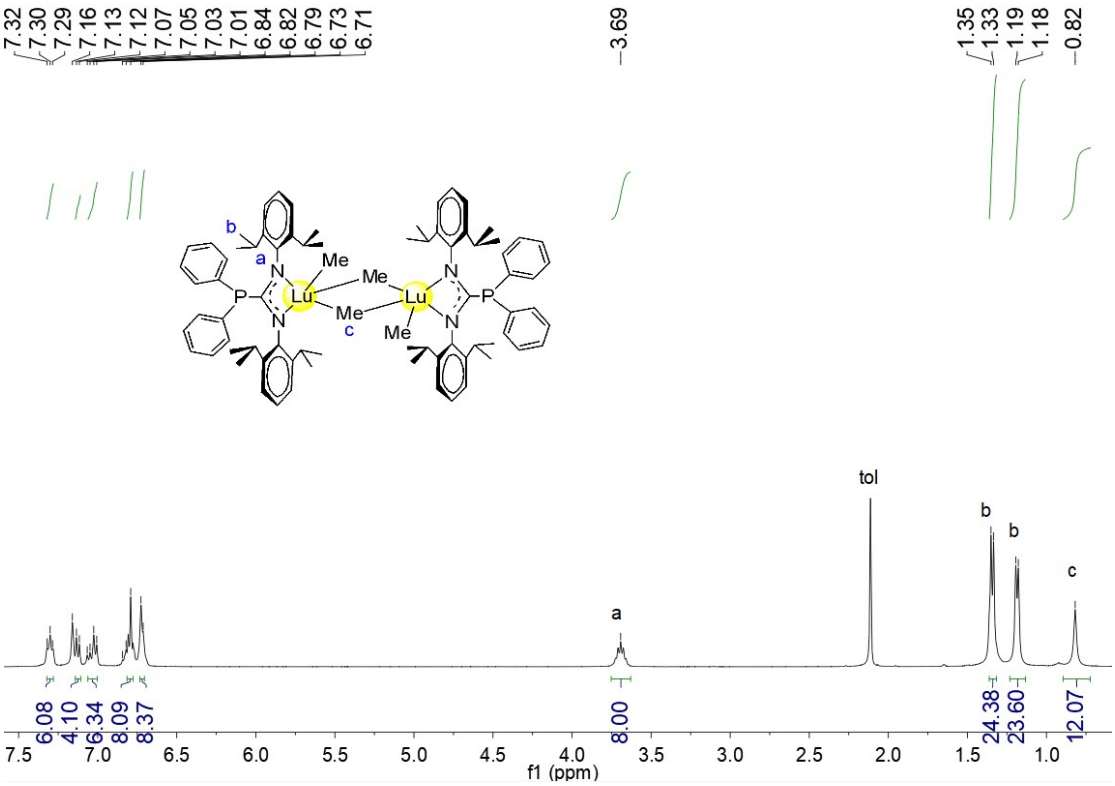

Figure S15. ^{1}H NMR spectrum of **4** obtained in C_6D_6 at room temperature.

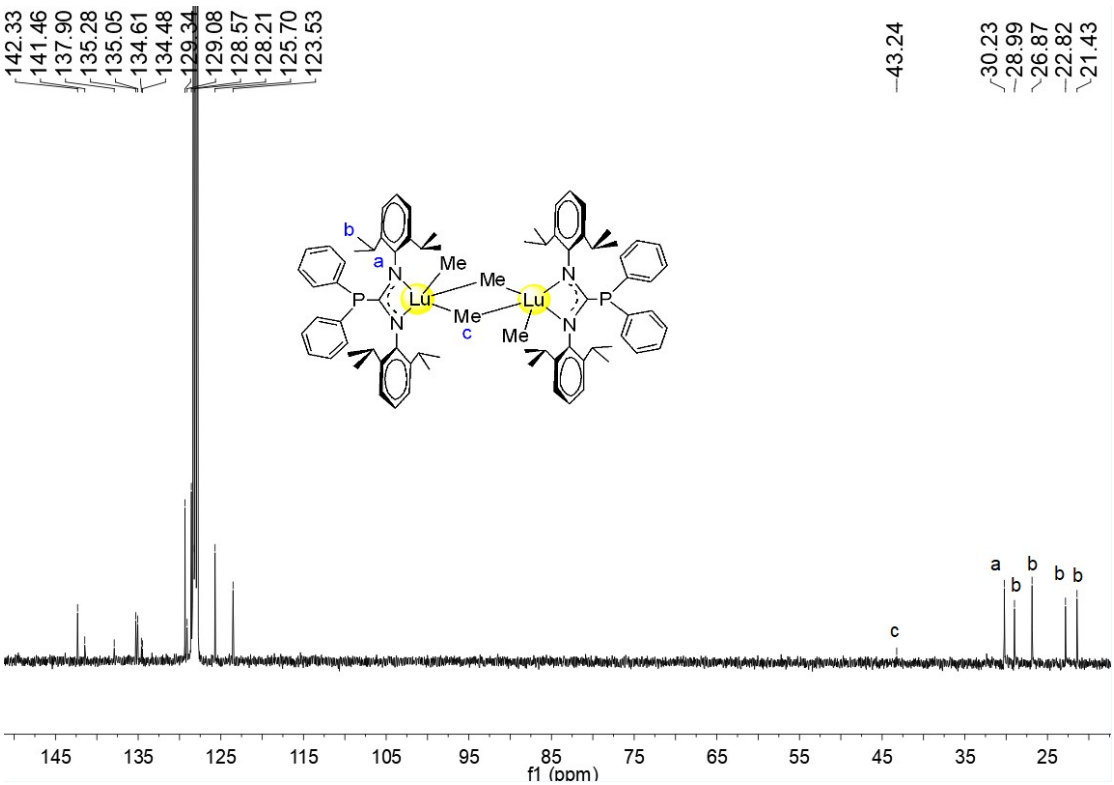

Figure S16. $^{13}C\{^{1}H\}$ NMR spectrum of **4** obtained in C_6D_6 at room temperature.

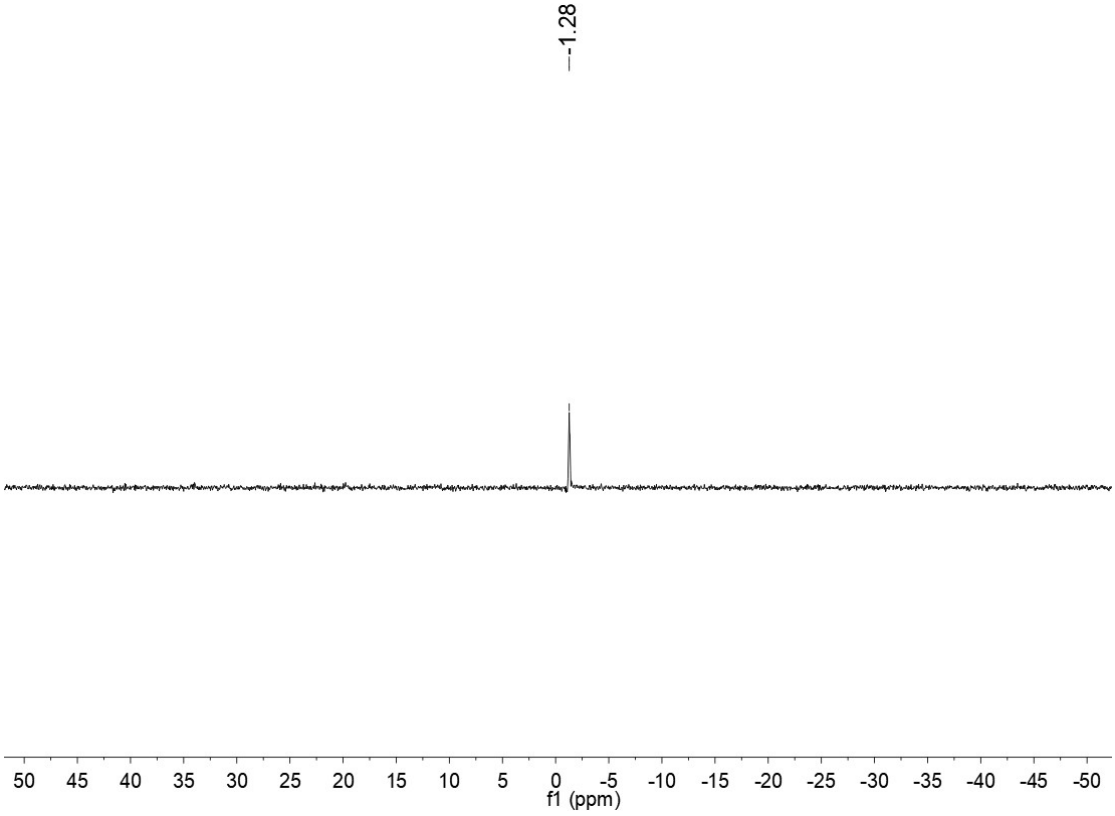

Figure S17. $^{31}P\{^{1}H\}$ NMR spectrum of **4** obtained in C_6D_6 at room temperature.

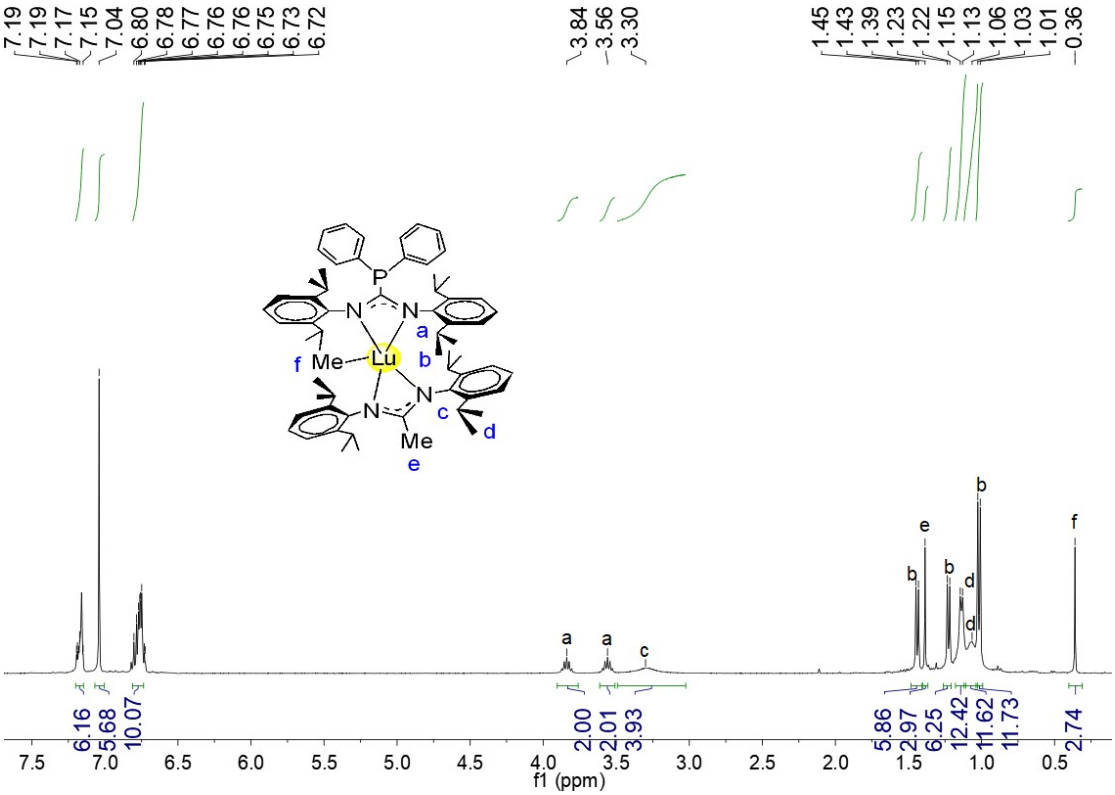

Figure S18. ^{1}H NMR spectrum of **5** obtained in C_6D_6 at room temperature.

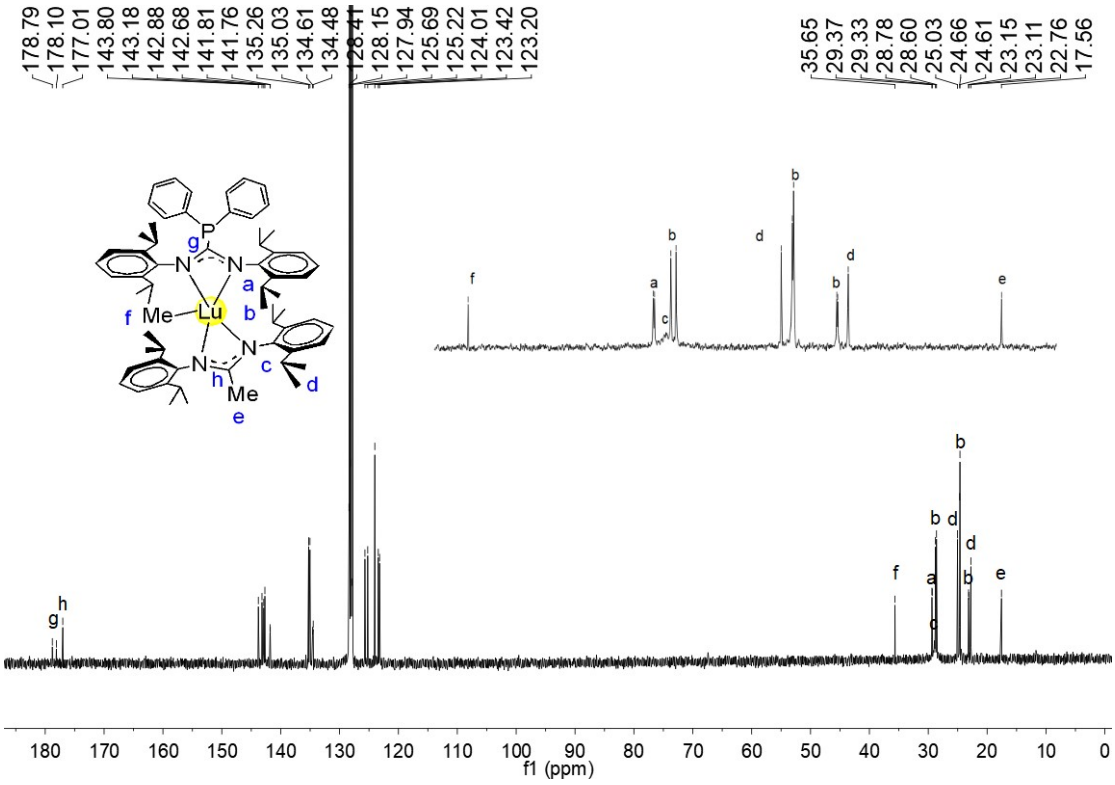

Figure S19. $^{13}C\{^{1}H\}$ NMR spectrum of **5** obtained in C_6D_6 at room temperature.

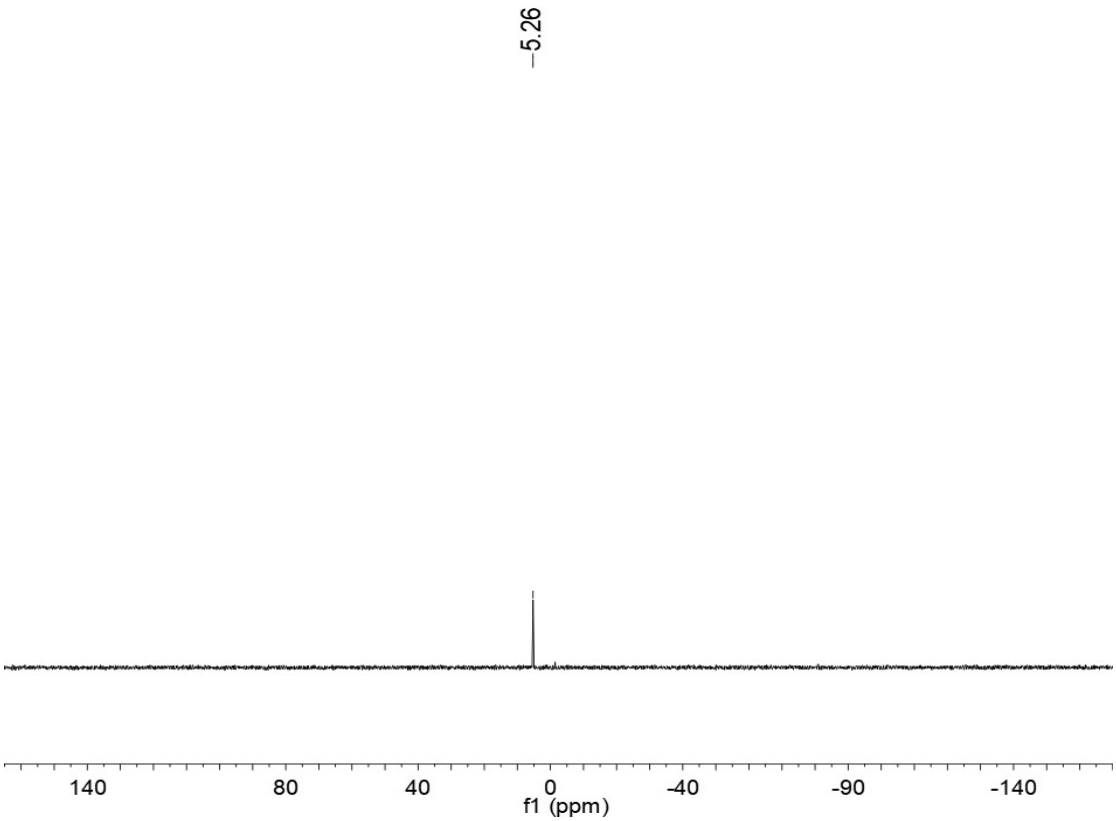

Figure S20. $^{31}P\{^{1}H\}$ NMR spectrum of **5** obtained in C_6D_6 at room temperature.

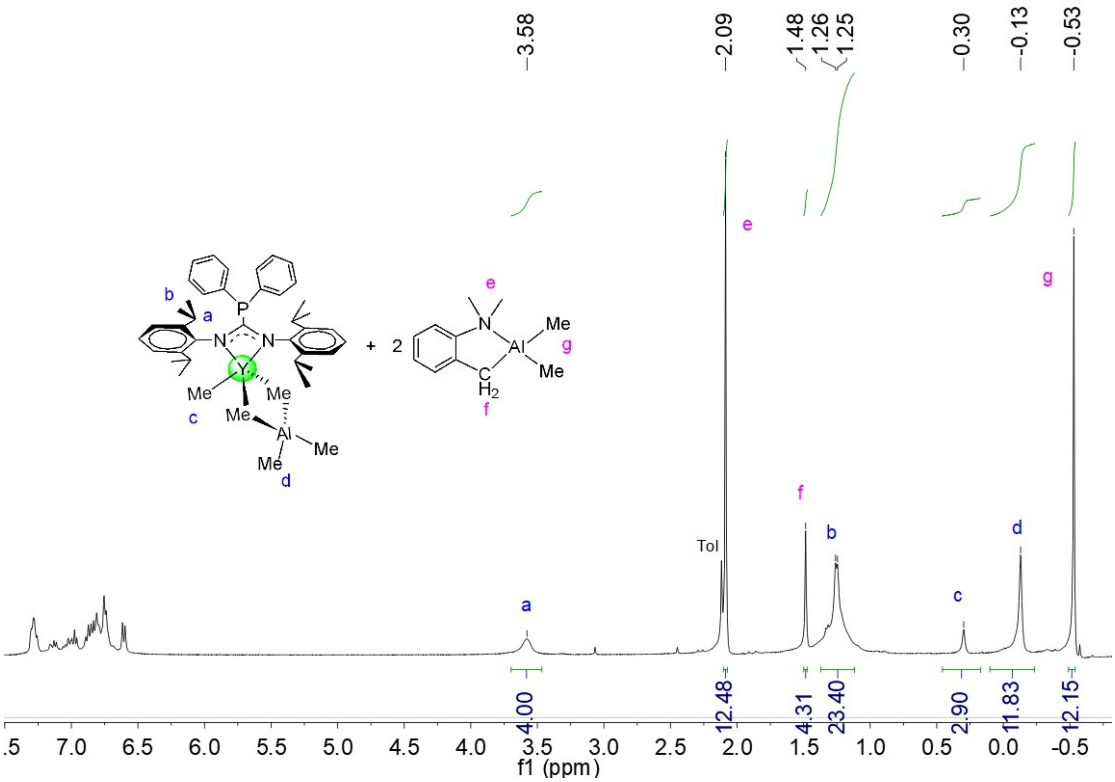

Figure S21. The *in situ* ^{1}H NMR spectrum of **6-Y** obtained in C_6D_6 at room temperature.

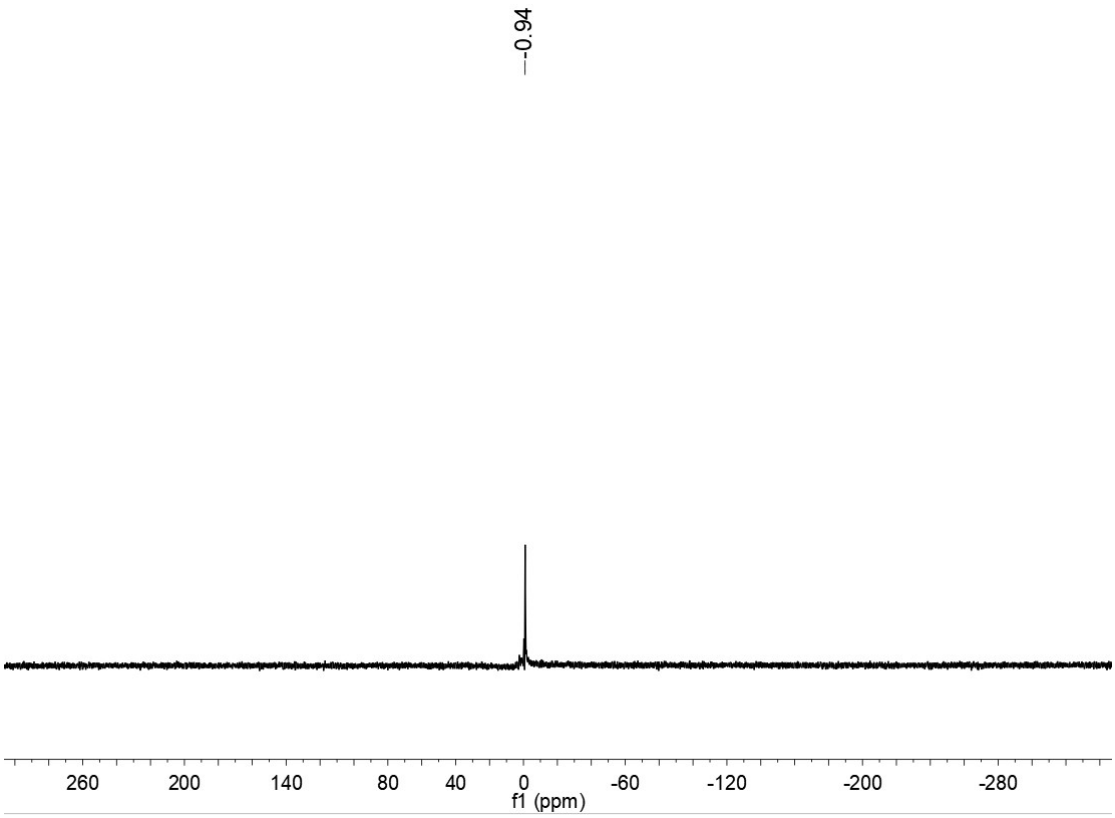

Figure S22. The *in situ* $^{31}P\{^{1}H\}$ NMR spectrum of **6-Y** obtained in C_6D_6 at room temperature.

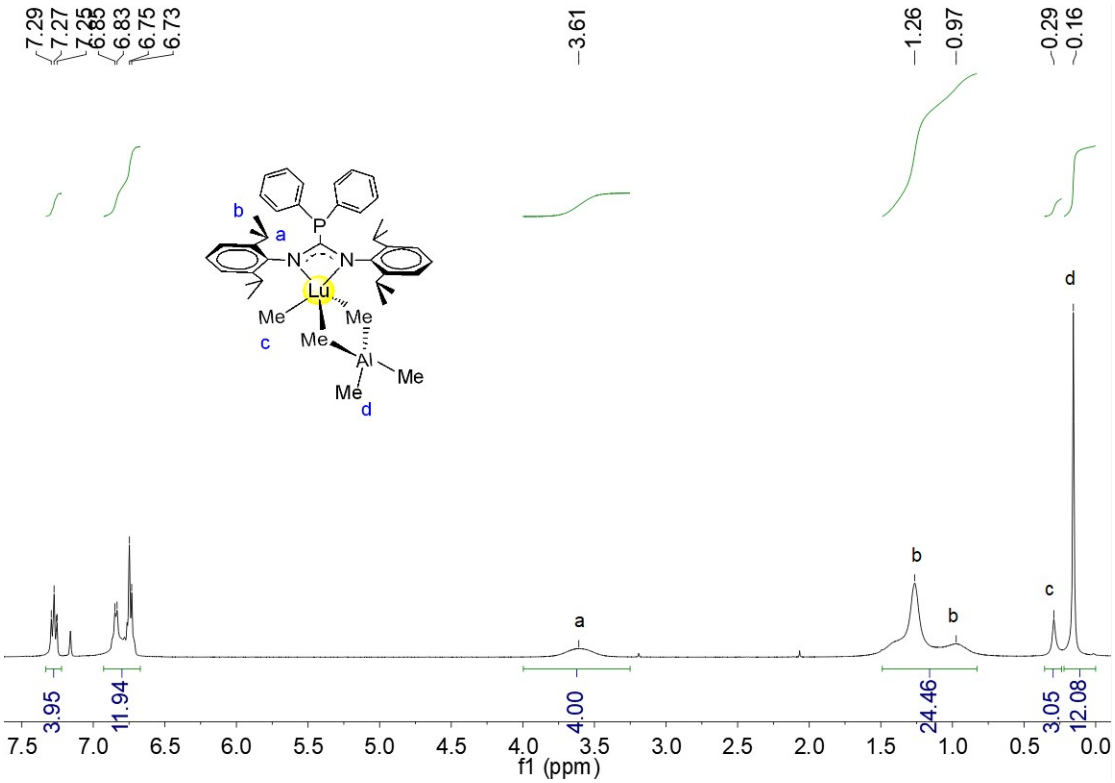

Figure S23. ^{1}H NMR spectrum of **6-Lu** obtained in C_6D_6 at room temperature.

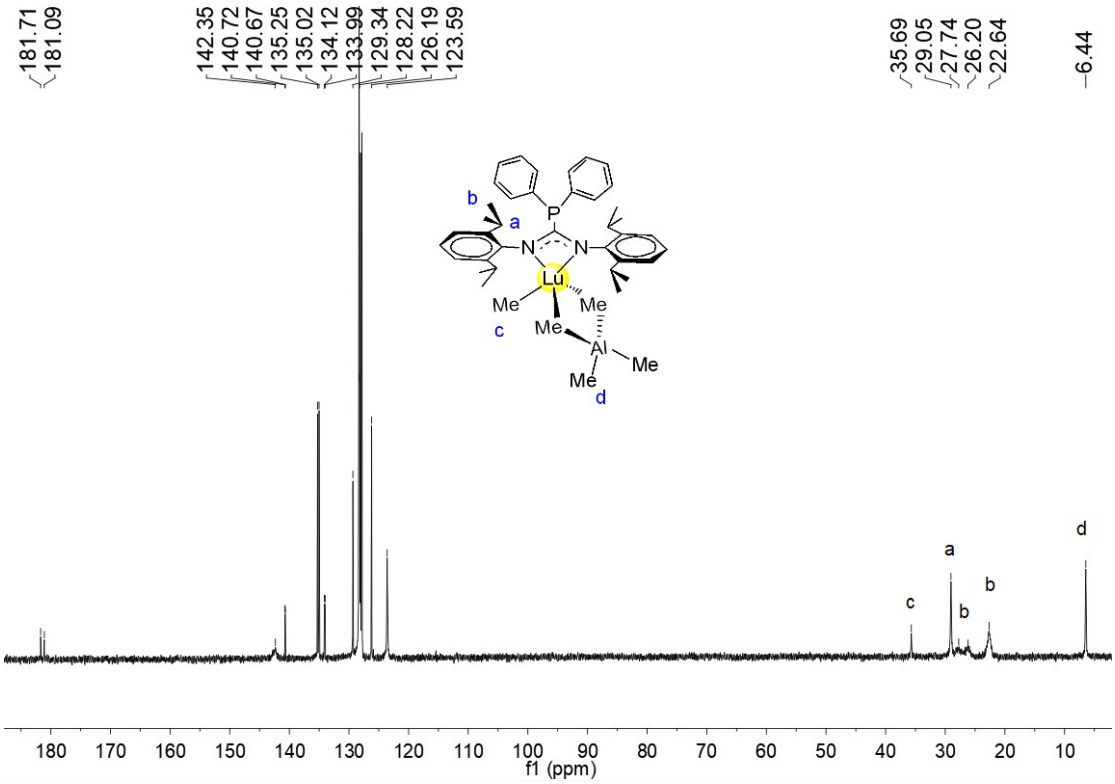

Figure S24. $^{13}C\{^{1}H\}$ NMR spectrum of **6-Lu** obtained in C_6D_6 at room temperature.

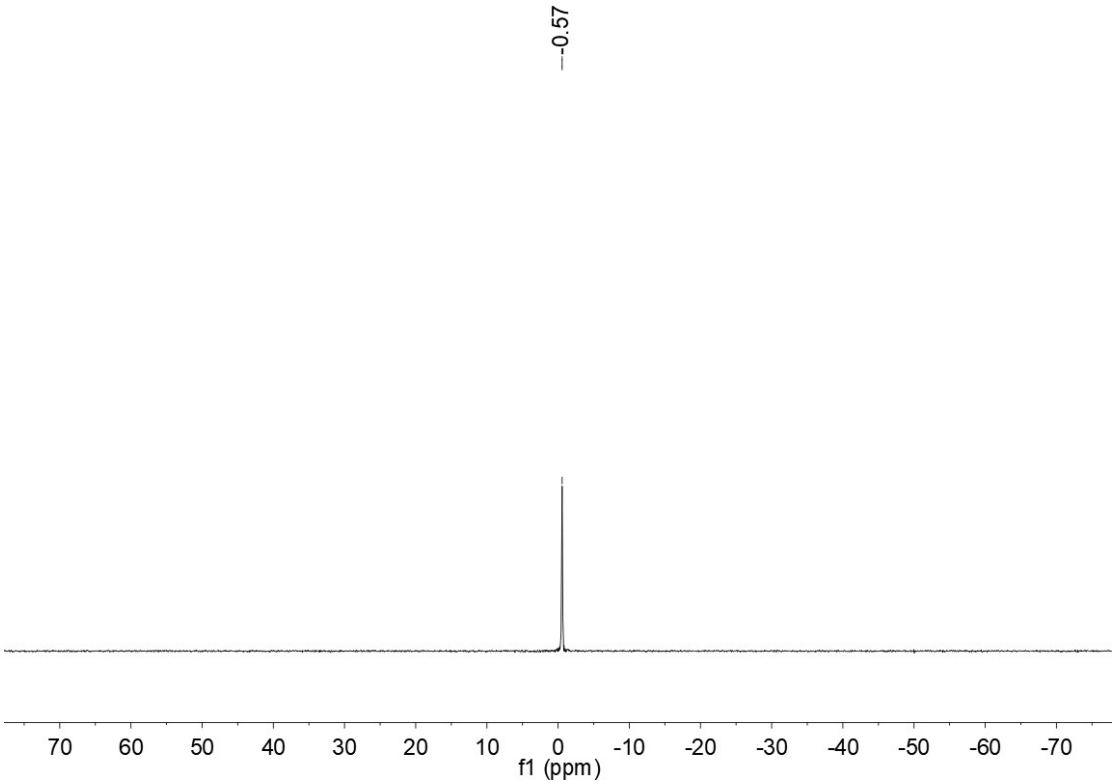

Figure S25. $^{31}P\{^{1}H\}$ NMR spectrum of **6-Lu** obtained in C_6D_6 at room temperature.

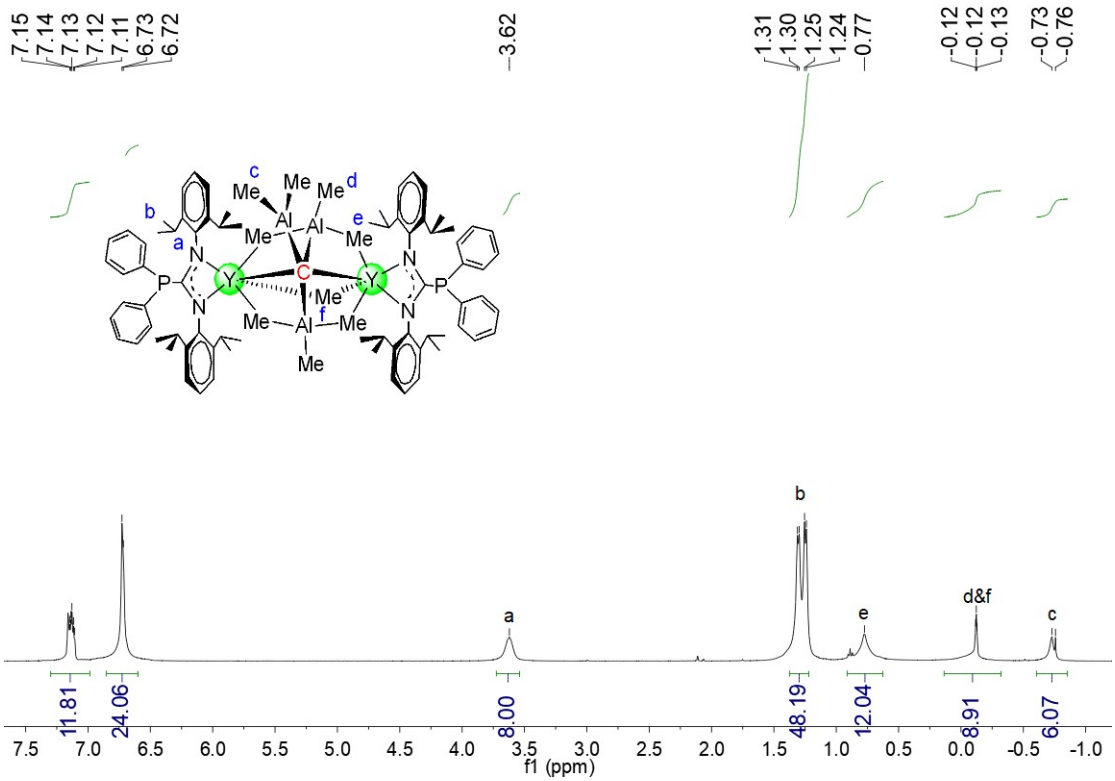

Figure S26. ^{1}H NMR spectrum of **8** obtained in C_6D_6 at room temperature.

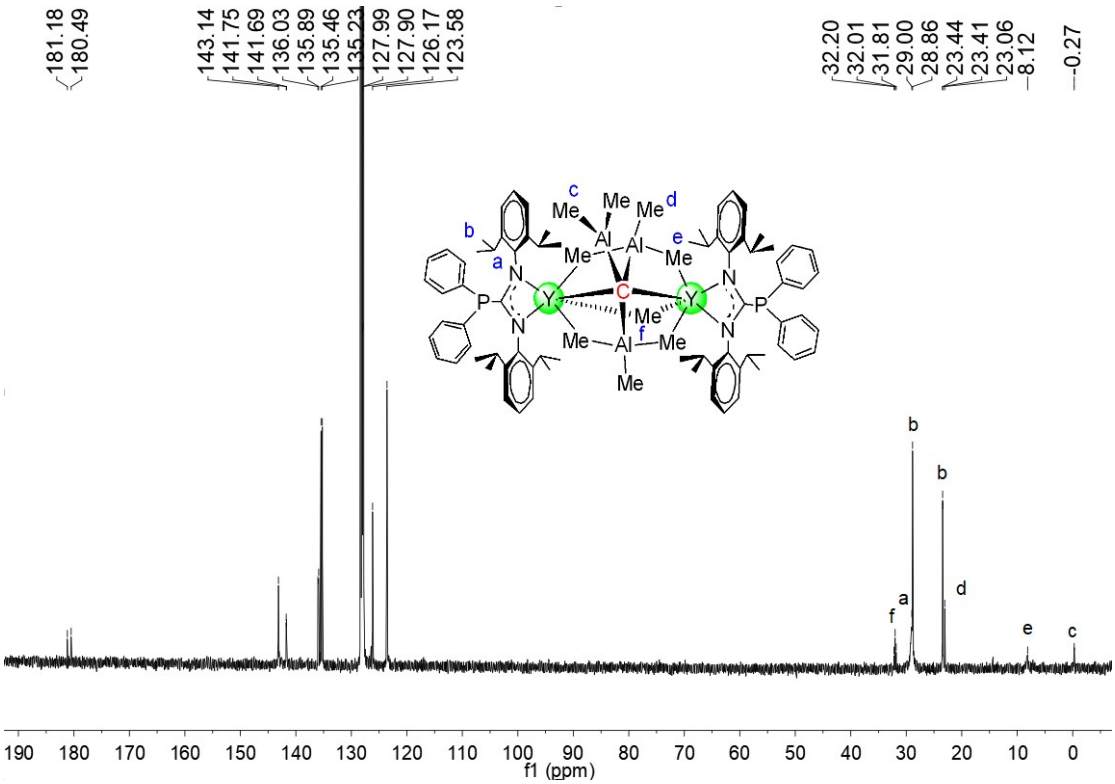

Figure S27. $^{13}C\{^{1}H\}$ NMR spectrum of **8** obtained in C_6D_6 at room temperature.

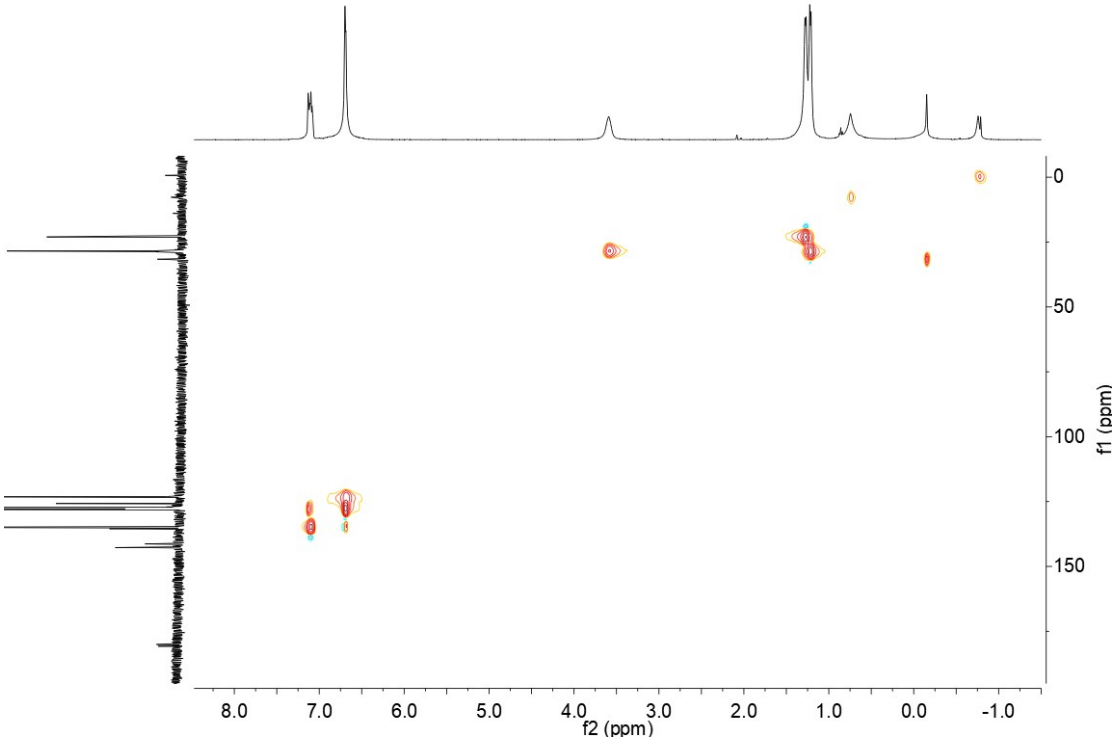

Figure S28. Two-dimensional ^{1}H-^{13}C HMQC NMR spectrum of complex **8** (^{1}H NMR spectrum (400 MHz) on the top, $^{13}C\{^{1}H\}$ NMR spectrum (100 MHz) on the left).

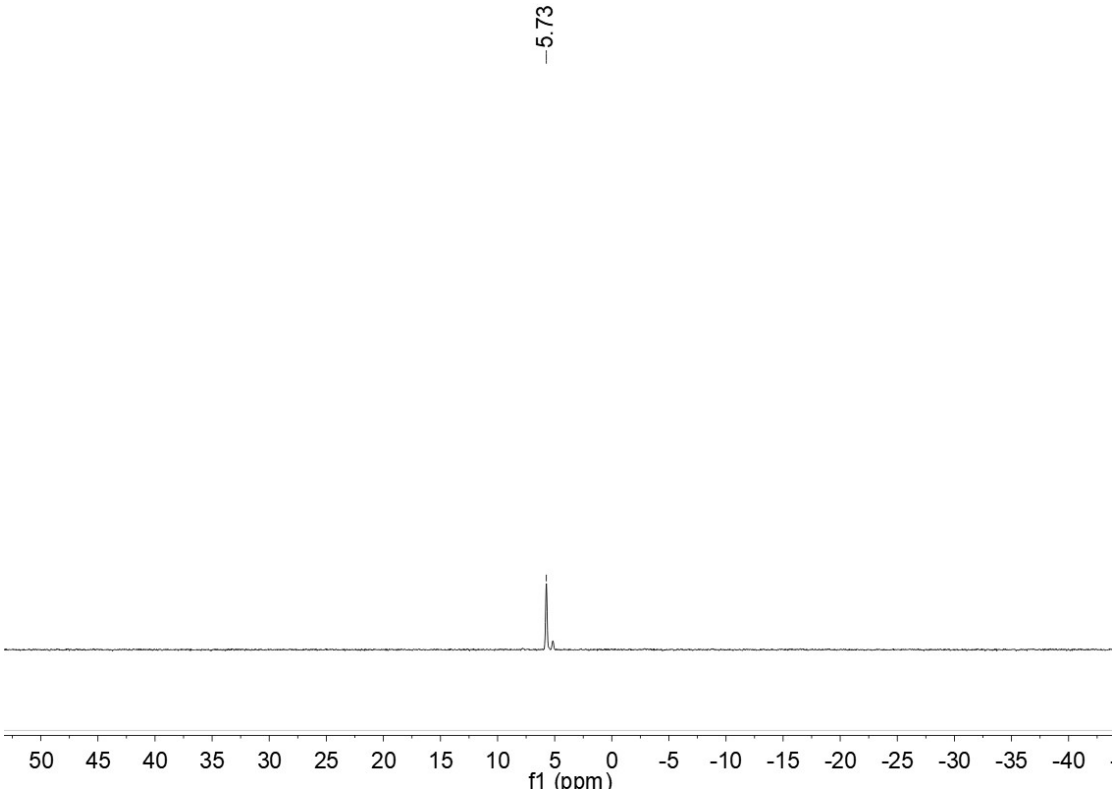

Figure S29. $^{31}P\{^{1}H\}$ NMR spectrum of **8** obtained in C_6D_6 at room temperature.

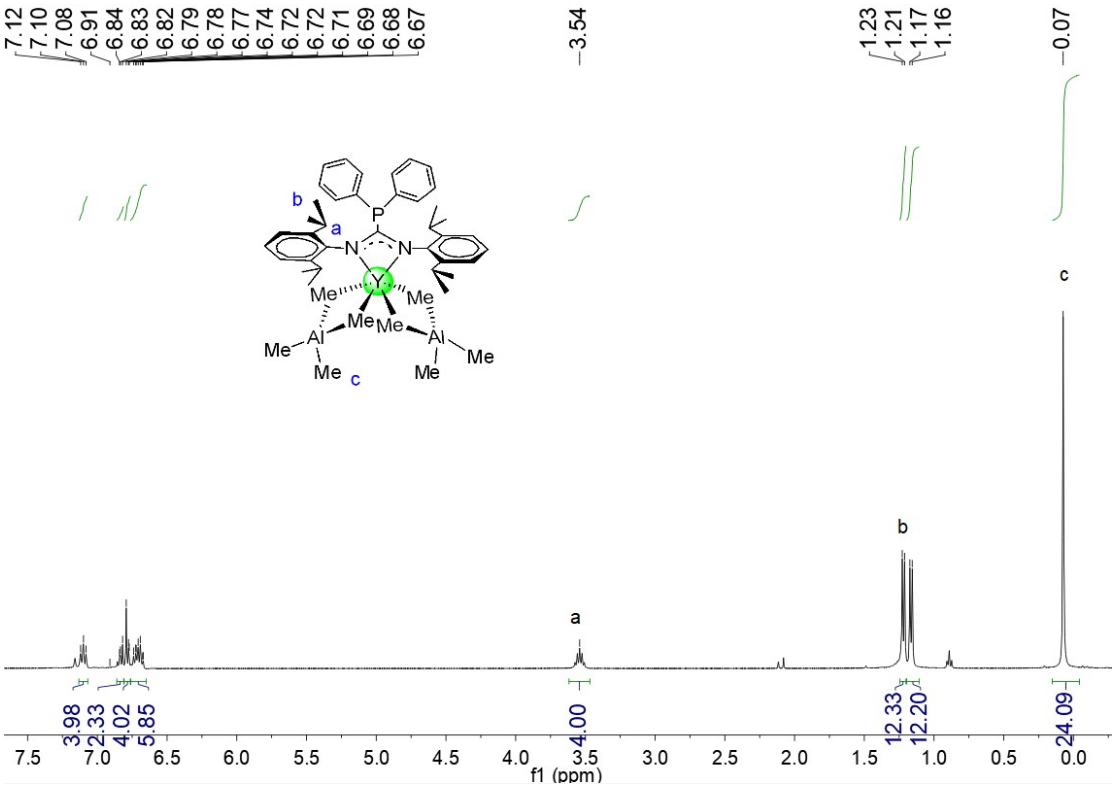

Figure S30. ^{1}H NMR spectrum of **9** obtained in C_6D_6 at room temperature.

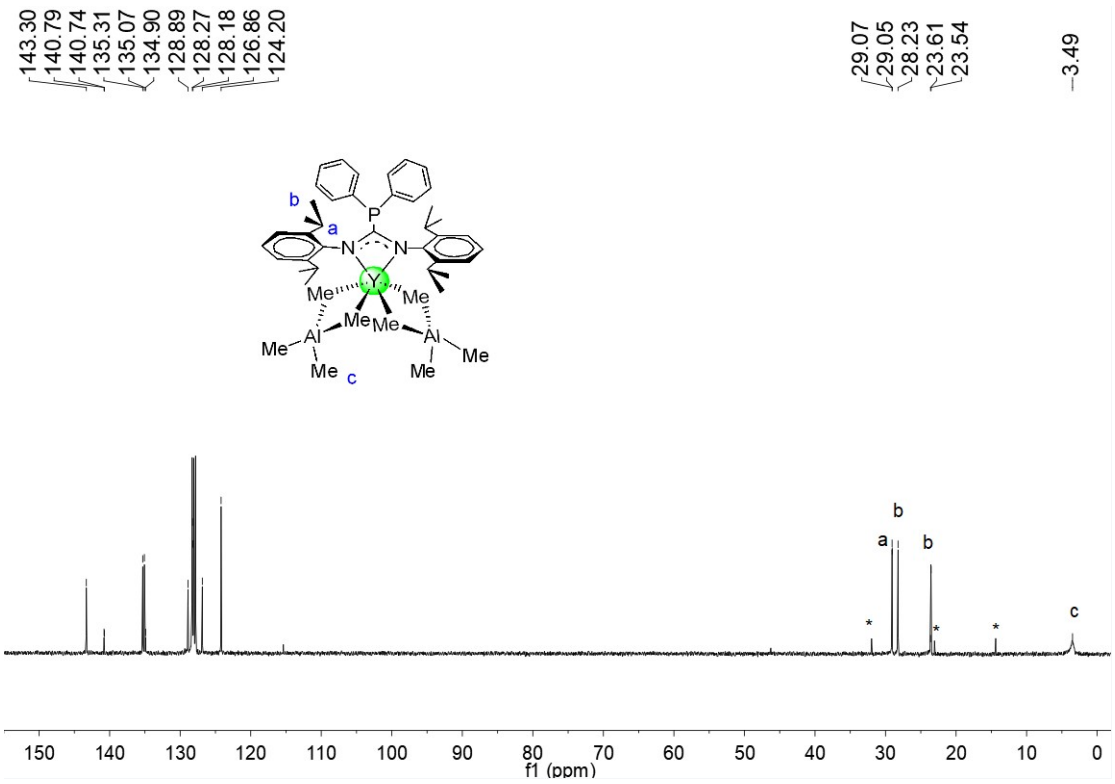

Figure S31. $^{13}C\{^{1}H\}$ NMR spectrum of **9** obtained in C_6D_6 at room temperature.

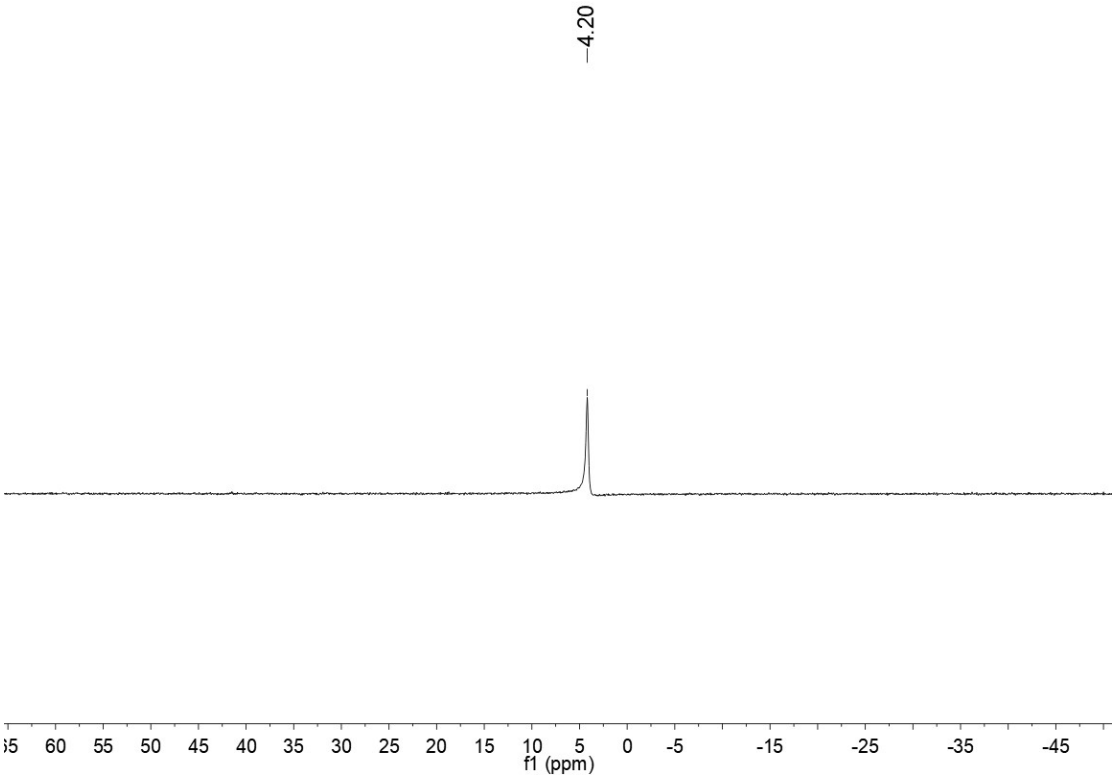

Figure S32. $^{31}P\{^{1}H\}$ NMR spectrum of **9** obtained in C_6D_6 at room temperature.

X-ray Crystallographic structure determinations

All crystals for X-ray analysis were obtained as described in the preparations. Suitable crystals were sealed in the thin-wall glass capillaries under a microscope in the glovebox. Data collections were performed on a Bruker SMART APEX or Bruker SMART APEX II (at 173 K or 296 K) diffractometer with CCD area detector using graphite-monochromated Mo/Ga Kα radiation (λ = 0.71073 Å / λ = 1.34138 Å). The determination of crystal class and unit cell was carried out by using the SMART program package. The raw frame data were processed using SAINT[2] and SADABS[3] to yield the reflection data file. The structure was solved by using the SHELXTL program[4] Refinement was performed on F^2 anisotropically by the full-matrix least-squares method for all the non-hydrogen atoms. The analytical scattering factors for neutral atoms were used throughout the analysis. Except for the hydrogen atoms on bridging carbons, hydrogen atoms were placed at the calculated positions and included in the structure calculation without further refinement of the parameters. The hydrogen atoms on bridging carbons were located by difference Fourier syntheses and their coordinates and isotropic parameters were refined. The residual electron densities were of no chemical significance. Crystal data, data collection, and processing parameters: 2389279 (for **1-Y**), 2389282 (for **1-Lu**), 2389309 (for **2**), 2389276 (for **4**), 2389280 (for **5**), 2389278 (for **6-Lu**), 2389281 (for **7**), 2389283 (for **8**) and 2389277 (for **9**) contain the supplementary crystallographic data for this paper. These data can be obtained free of charge from The Cambridge Crystallographic Data Centre *via* www.ccdc.cam.ac.uk/ datarequest/cif.

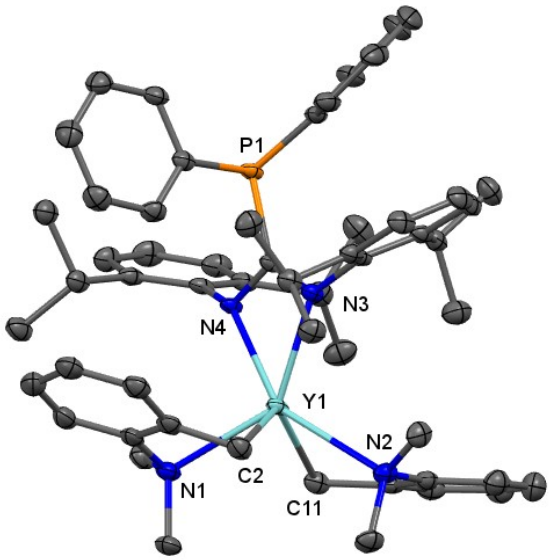

Figure S33. Molecular structure of complex **1-Y** with thermal ellipsoids at 30% probability. All hydrogen atoms are omitted for clarity. Selected bond lengths (Å) and angles (deg): Y(1)-C(2) 2.441(3), Y(1)-C(11) 2.436(3), Y(1)-N(1) 2.524(2), Y(1)-N(2) 2.607(2), Y(1)-N(3) 2.403(2), Y(1)-N(4) 2.475(2); C(2)-Y(1)-N(1) 68.47(8), N(1)-Y(1)-N(2) 117.76(7), N(1)-Y(1)-C(11) 84.57(9), N(2)-Y(1)-C(11) 67.32(8), C(2)-Y(1)-N(2) 81.04(8), C(2)-Y(1)-C(11) 121.88(10).

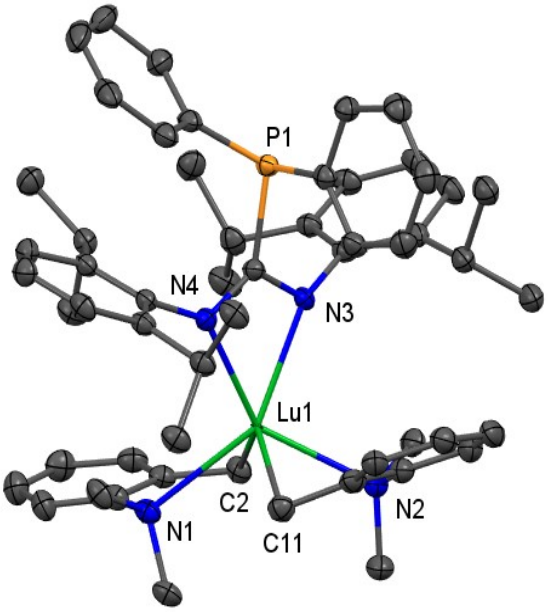

Figure S34. Molecular structure of complex **1-Lu** with thermal ellipsoids at 30% probability. All hydrogen atoms are omitted for clarity. Selected bond lengths (Å) and angles (deg): Lu(1)-C(2) 2.381(5), Lu(1)-C(11) 2.396(5), Lu(1)-N(2) 2.487(4), Lu(1)-N(1) 2.559(4), Lu(1)-N(3) 2.358(4), Lu(1)-N(4) 2.427(4); C(2)-Lu(1)-N(1) 68.39(15), N(1)-Lu(1)-N(2) 119.28(14), N(1)-Lu(1)-C(11) 81.93(16), N(2)-Lu(1)-C(11) 69.21(17), C(2)-Lu(1)-N(2) 85.23(17), C(2)-Lu(1)-C(11) 124.08(19).

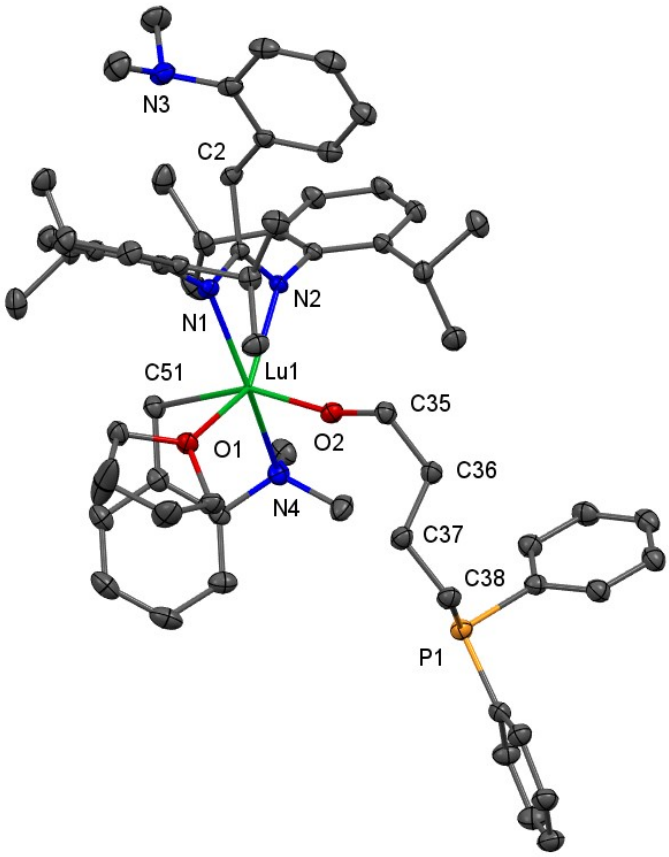

Figure S35. Molecular structure of complex **2** with thermal ellipsoids at 30% probability. All hydrogen atoms are omitted for clarity. Selected bond lengths (Å) and angles (deg): Lu(1)-N(1) 2.299(4), Lu(1)-N(2) 2.347(3), Lu(1)-N(4) 2.535(4), Lu(1)-O(2) 2.044(3), Lu(1)-O(1) 2.316(3), Lu(1)-C(51) 2.476(5); N(1)-Lu(1)-O(2) 107.70(13), N(2)-Lu(1)-O(2) 101.95(13), N(1)-Lu(1)-C(51) 95.68(15), N(2)-Lu(1)-C(51) 95.07(15), N(1)-Lu(1)-O(1) 88.49(12), N(2)-Lu(1)-O(1) 146.07(12).

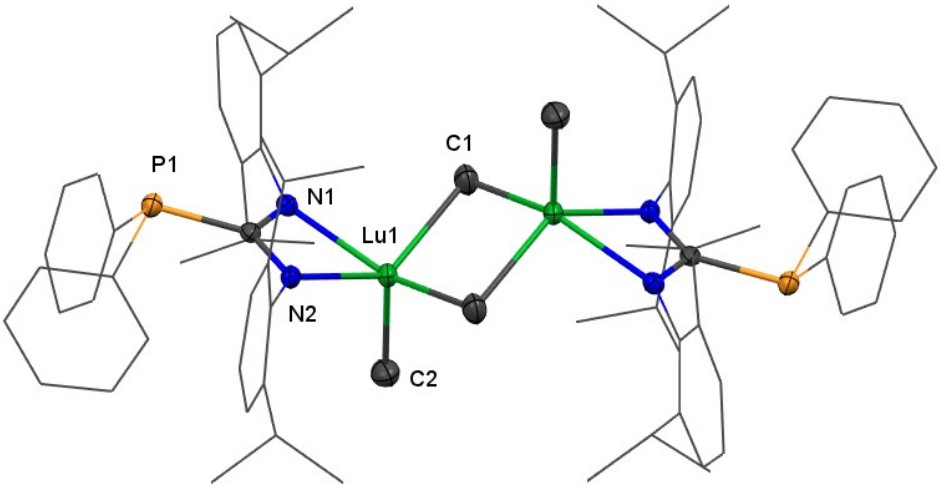

Figure S36. Molecular structure of complex **4** with thermal ellipsoids at 30% probability except for the 2,6-(^{i}Pr)$_2$C$_6$H$_3$ groups and phenyl groups in the phosphaguanidinate ligand. All hydrogen atoms are omitted for clarity. Selected bond lengths (Å) and angles (deg): Lu(1)-Lu(1A) 3.3824(5), Lu(1)-N(1) 2.284(4), Lu(1)-N(2) 2.290(4), Lu(1)-C(1) 2.441(6), Lu(1)-C(1A) 2.428(6), Lu(1)-C(2) 2.297(6); N(1)-Lu(1)-N(2) 58.58(14), N(1)-Lu(1)-C(1) 141.64(19), N(1)-Lu(1)-C(2) 109.12(19), N(2)-Lu(1)-C(1) 93.35(17), N(2)-Lu(1)-C(2) 111.70(18), C(1)-Lu(1)-C(2) 105.4(2), C(1A)-Lu(1)-C(2) 110.7(2).

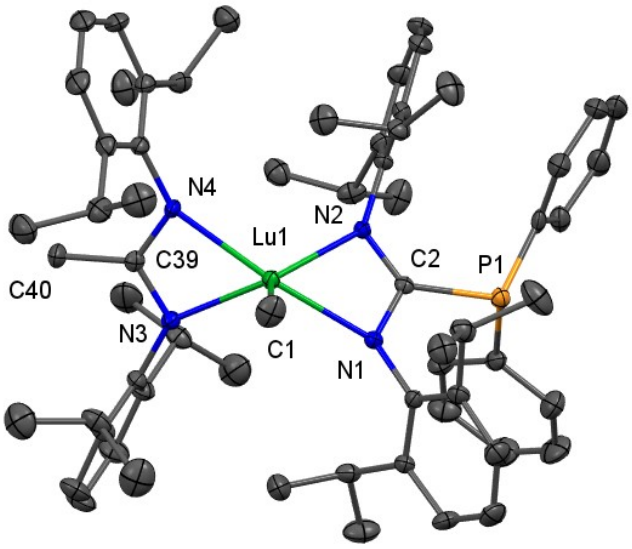

Figure S37. Molecular structure of complex **5** with thermal ellipsoids at 30% probability. All hydrogen atoms are omitted for clarity. Selected bond lengths (Å) and angles (deg): Lu(1)-N(1) 2.305(3), Lu(1)-N(2) 2.316(3), Lu(1)-N(3) 2.244(3), Lu(1)-N(4) 2.308(3), Lu(1)-C(1) 2.308(4), C(39)-C(40) 1.501(5), C(2)-P(1) 1.878(4); N(1)-Lu(1)-C(1) 93.43(15), N(2)-Lu(1)-C(1) 127.61(16), N(3)-Lu(1)-C(1) 107.38(16), N(4)-Lu(1)-C(1) 102.68(15), N(1)-Lu(1)-N(2) 57.84(11), N(3)-Lu(1)-N(4) 59.17(11).

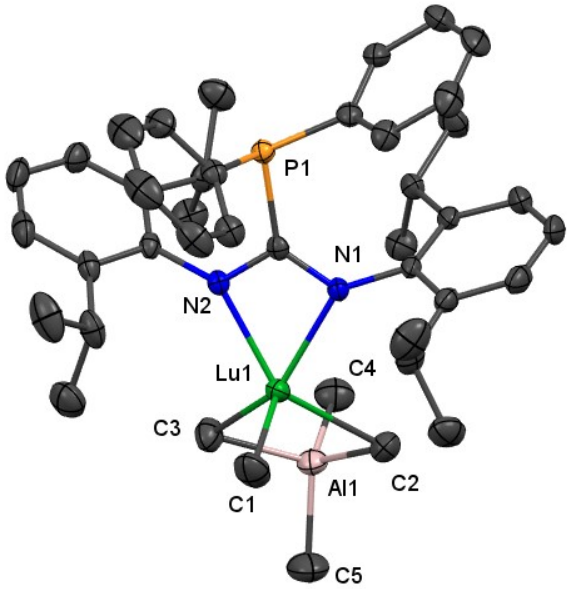

Figure S38. Molecular structure of complex **6-Lu** with thermal ellipsoids at 30% probability. All hydrogen atoms are omitted for clarity. Selected bond lengths (Å) and angles (deg): Lu(1)-C(1) 2.307(3), Lu(1)-C(2) 2.472(4), Lu(1)-C(3) 2.431(4), Al(1)-C(4) 1.959(3), Lu(1)-N(1) 2.276(2), Lu(1)-N(2) 2.273(2); C(1)-Lu(1)-N(1) 112.43(11), C(1)-Lu(1)-N(2) 111.55(11), C(1)-Lu(1)-C(2) 102.93(13), C(1)-Lu(1)-C(3) 105.83(14).

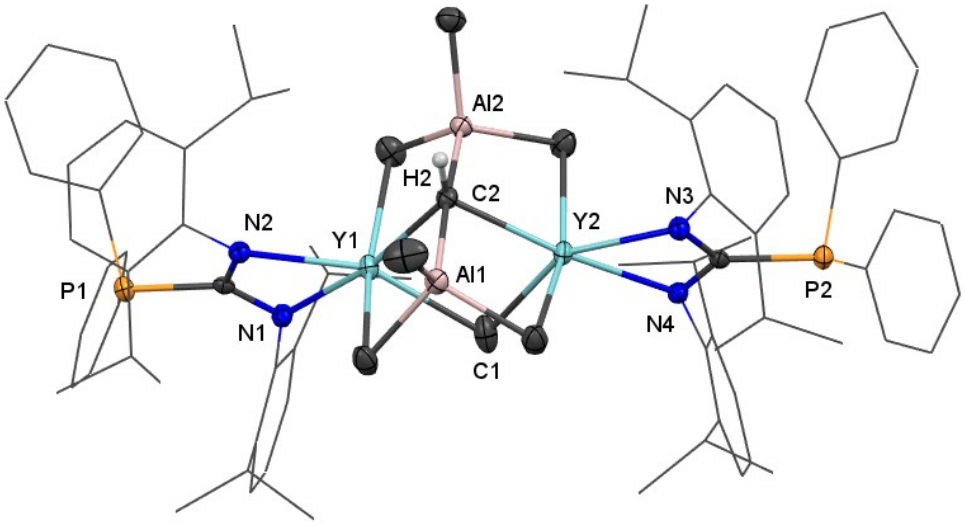

Figure S39. Molecular structure of complex **7** with thermal ellipsoids at 30% probability except for the 2,6-(^{i}Pr)$_2$C$_6$H$_3$ groups and phenyl groups in the phosphaguanidinate ligand. All hydrogen atoms are omitted for clarity (except for H2). Selected bond lengths (Å) and angles (deg): Y(1)-C(1) 2.538(3), Y(1)-C(2) 2.390(2), Y(2)-C(1) 2.508(3), Y(2)-C(2) 2.414(2), C(2)-Al(1) 1.992(3), C(2)-Al(2) 1.983(3), Y(1)-C(3) 2.593(3), Y(1)-C(6) 2.646(3), Y(2)-C(5) 2.601(3), Y(2)-C(8) 2.609(3); C(1)-Y(1)-C(2) 85.28(9), C(1)-Y(2)-C(2) 85.42(9), Y(1)-C(1)-Y(2) 91.50(11), Y(1)-C(2)-Y(2) 97.58(8).

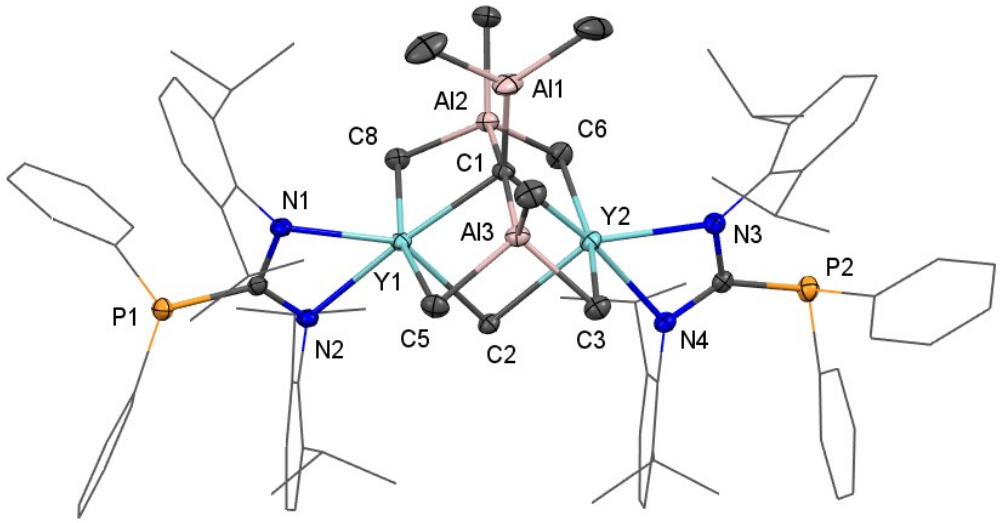

Figure S40. Molecular structure of complex **8** with thermal ellipsoids at 30% probability except for the 2,6-(^{i}Pr)$_2$C$_6$H$_3$ groups and phenyl groups in the phosphaguanidinate ligand. All hydrogen atoms are omitted for clarity. Selected bond lengths (Å) and angles (deg): Y(1)-Y(2) 3.6371(5), Y(1)-C(1) 2.429(3), Y(1)-C(2) 2.597(3), Y(1)-C(5) 2.574(3), Y(1)-C(8) 2.562(3), Y(2)-C(3) 2.620(3), Y(2)-C(6) 2.583(3), Y(2)-C(1) 2.421(3), Y(2)-C(2) 2.566(2), C(1)-Al(1) 1.939(3), C(1)-Al(2) 1.973(3), C(1)-Al(3) 1.972(3); C(1)-Y(1)-C(2) 86.18(9), C(1)-Y(2)-C(2) 87.05(9), Y(1)-C(1)-Y(2) 97.17(9), Y(1)-C(2)-Y(2) 89.57(8), Al(1)-C(1)-Al(2) 93.82(12), Al(1)-C(1)-Al(3) 96.52(12), Al(2)-C(1)-Al(3) 169.63(15).

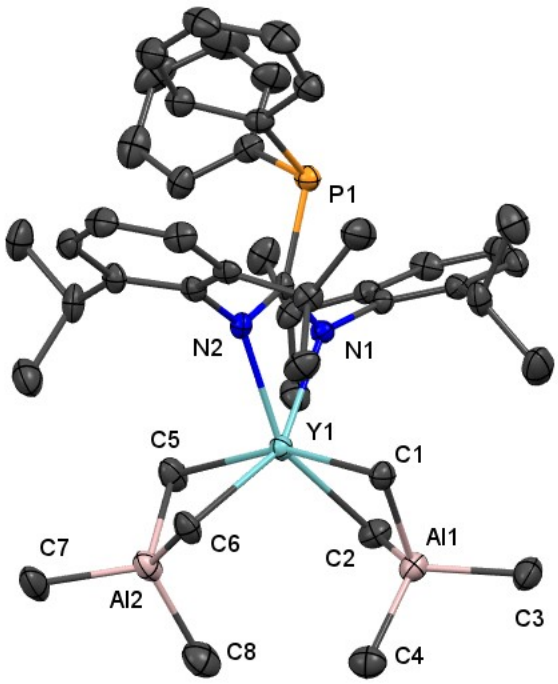

Figure S41. Molecular structure of complex **9** with thermal ellipsoids at 30% probability. All hydrogen atoms are omitted for clarity. Selected bond lengths (Å) and angles (deg): Y(1)-N(1) 2.326(4), Y(1)-N(2) 2.351(4), Y(1)-C(1) 2.528(4), Y(1)-C(2) 2.558(4), Y(1)-C(5) 2.541(4), Y(1)-C(6) 2.570(4); C(1)-Y(1)-N(1) 103.90(11), C(1)-Y(1)-N(2) 97.65(11), C(2)-Y(1)-N(1) 94.93(12), C(2)-Y(1)-N(2) 150.89(13), C(5)-Y(1)-N(1) 96.19(11), C(5)-Y(1)-N(2) 99.99(12), C(6)-Y(1)-N(1) 151.81(13), C(6)-Y(1)-N(2) 95.77(12), C(1)-Y(1)-C(2) 79.89(13), C(5)-Y(1)-C(6) 79.65(13).

Table S1. Crystal data and refinement details of complexes **1-Y, 1-Lu** and **2**

	1-Y	**1-Lu**	**2**
Formula	$C_{55}H_{68}N_4PY$	$C_{55}H_{68}N_4PLu$	$C_{63}H_{84}LuN_4O_2P$
Molecular weight	905.01	991.07	1135.28
Crystal system	Monoclinic	Monoclinic	Triclinic
Space group	$P2_1/n$	$P2_1/n$	P-1
a /(Å)	15.5692(14)	15.5704(6)	10.7810(7)
b/ (Å)	18.5082(16)	18.4527(6)	12.3125(8)
c/ (Å)	16.5373(15)	16.5098(6)	23.2922(15)
V/ (Å^3)	4722.5(7)	4698.0(3)	4305.7(5)
Z	4	4	2
ρ_c /(mg. m^{-3})	1.273	1.401	1.321
μ(Mo-K_α)/(mm^{-1})	1.568	3.058	2.577
Limiting indices	-18<=h<=18, -22<=k<=22, -19<=l<=19	-19<=h<=19, -22<=k<=23, -20<=l<=20	-12<=h<=12, -14<=k<=14, -27<=l<=27
Collected reflections	53122	71428	72131
Unique	8349 [R(int)= 0.1093]	10102 [R(int)= 0.1177]	10086 [R(int) = 0.0701]
Parameters	570	562	652
Goodness of fit on F^2	1.043	1.053	1.219
R_1[a],wR_2[a][I >2σ(I)]	R_1 = 0.0439 wR_2 = 0.1111	R_1 = 0.0613 wR_2 = 0.1596	R_1 = 0.0445 wR_2 = 0.1166
R_1, wR_2indices (all data)	R_1 = 0.0519 wR_2 = 0.1178	R_1 = 0.0712 wR_2 = 0.1659	R_1 = 0.0466 wR_2 = 0.1174
Max/min residual density(e Å^{-3})	1.00 and -0.51	1.27 and -2.19	0.90 and -1.00

[a]R1 = ∑|| F0|-|F_c|| (based on reflections with $F_o^2 > 2\sigma F^2$). wR_2 = [∑ [w(F_o^2-F_c^2)^2]/ ∑[w(F_o^2)^2]]$^{1/2}$; w = 1/[σ^2(F_o^2) + (0.095P)^2]; P = [max(F_o^2, 0) +2F_c^2]/3 (also with F_o^2 > 2σF^2).

Table S2. Crystal data and refinement details of complexes **4, 5** and **6-Lu**

	4	**5**	**6-Lu**
Formula	$C_{92}H_{110}Lu_2N_4P_2$	$C_{64}H_{85}LuN_4P$	$C_{42}H_{59}AlLuN_2P$
Molecular weight	1683.72	1116.29	824.83
Crystal system	Triclinic	Monoclinic	Monoclinic
Space group	*P*-1	$P2_1/c$	$P2_1/n$
a /(Å)	10.5399(4)	12.962(8)	12.7487(5)
b/ (Å)	11.7073(5)	19.845(8)	18.7568(7)
c/ (Å)	19.0482(8)	22.439(7)	17.9516(7)
V/ (Å^3)	2094.24(15)	5704(6)	4288.6(3)
Z	2	4	4
ρ_c /(mg. m^{-3})	1.340	1.300	1.277
μ(Mo-K$_\alpha$)/(mm^{-1})	2.427	1.801	2.388
Limiting indices	-12<=h<=12, -13<=k<=13, -22<=l<=22	-15<=h<=15, -23<=k<=23, -25<=l<=26	-14<=h<=15, -22<=k<=22, -21<=l<=21
Collected reflections	44234	59596	45965
Unique	7409 [R(int)= 0.0544]	10112 [R(int)= 0.0817]	7578 [R(int) = 0.0436]
Parameters	473	649	459
Goodness of fit on F^2	1.200	1.051	1.100
R_1[a],wR_2[a][I >2σ(I)]	R_1 = 0.0372 wR_2 = 0.0803	R_1 = 0.0320 wR_2 = 0.0654	R_1 = 0.0218 wR_2 = 0.0438
R_1, wR_2indices (all data)	R_1 = 0.0430 wR_2 = 0.0829	R_1 = 0.0566 wR_2 = 0.0778	R_1 = 0.0313 wR_2 = 0.0500
Max/min residual density(e Å^{-3})	1.45 and -1.54	0.91 and -0.90	0.33 and -0.79

[a] R1 = ∑|| F0|-|F_c|| (based on reflections with $F_o^2 > 2\sigma F^2$). $wR_2 = [\sum [w(F_o^2-F_c^2)^2]/\sum[w(F_o^2)^2]]^{1/2}$; $w = 1/[\sigma^2(F_o^2) + (0.095P)^2]$; $P = [\max(F_o^2, 0) + 2F_c^2]/3$ (also with $F_o^2 > 2\sigma F^2$).

Table S3. Crystal data and refinement details of complexes **7, 8** and **9**

	7	**8**	**9**
Formula	$C_{82}H_{110}Al_2N_4P_2Y_2$	$C_{84}H_{115}Al_3N_4P_2Y_2$	$C_{45}H_{68}Al_2N_2PY$
Molecular weight	1445.45	1501.49	810.85
Crystal system	Triclinic	Monoclinic	Monoclinic
Space group	*P*-1	$P2_1/n$	$P2_1/c$
a /(Å)	12.0176(6)	19.8360(19)	16.1150(14)
b/ (Å)	18.7006(11)	12.2333(12)	16.9001(16)
c/ (Å)	19.4040(11)	34.501(3)	19.322(2)
V/ (Å^3)	3899.7(4)	8352.7(14)	4872.5(8)
Z	2	4	4
ρ_c /(mg. m^{-3})	1.231	1.194	1.105
μ(Mo-K$_\alpha$)/(mm^{-1})	1.588	1.886	1.294
Limiting indices	-14<=h<=14 -22<=k<=22 -23<=l<=23	-23<=h<=23 -14<=k<=14 -41<=l<=41	-19<=h<=19 -20<=k<=20 -23<=l<=20
Collected reflections	85131	144943	41269
Unique	13652 [R(int) = 0.0978]	14774 [R(int) = 0.0756]	8614 [R(int) = 0.0943]
Parameters	911	930	520
Goodness of fit on F^2	1.044	1.029	1.038
R_1[a],wR_2[a][I >2σ(I)]	R_1 = 0.0363 wR$_2$ = 0.0798	R_1 = 0.0418 wR$_2$ = 0.0985	R_1 = 0.0464 wR$_2$ = 0.1078
R_1, wR_2indices (all data)	R_1 = 0.0533 wR$_2$ = 0.0867	R_1 = 0.0506 wR$_2$ = 0.1053	R_1 = 0.0776 wR$_2$ = 0.1208
Max/min residual density(e Å^{-3})	0.34 and -0.50	2.89 and -0.63	0.41 and -0.48

[a] R1 = ∑|| F0|-|F$_c$|| (based on reflections with $F_o^2 > 2\sigma F^2$). $wR_2 = [\sum [w(F_o^2-F_c^2)^2]/\sum[w(F_o^2)^2]]^{1/2}$; $w = 1/[\sigma^2(F_o^2) + (0.095P)^2]$; $P = [\max(F_o^2, 0) + 2F_c^2]/3$ (also with $F_o^2 > 2\sigma F^2$).

References

[1] J. Grundy, M. P. Coles, P. B. Hitchcock, *Dalton Trans.,* **2003**, 2573–2577; b) N. E. Mansfield, M. P. Coles, P. B. Hitchcock, *Dalton Trans.,* **2005**, 2833–2841.

[2] *SAINTPlus Data Reduction and Correction Program* v. 6.02a, Bruker AXS, Madison, WI, **2000**.

[3] G. M. Sheldrick, *SADABS*, A Program for Empirical Absorption Correction, University of Göttingen, Göttingen, Germany, **1998**.

[4] G. M. Sheldrick, *SHELXL-97*, Program for the Refinement of Crystal Structures, University of Göttingen, Göttingen, Germany, **1997**.